Outdoor thermal comfort autonomy: Performance metrics for climate-conscious urban design

Citation: Nazarian, Negin, Juan A. Acero and Leslie Norford. "Outdoor thermal comfort autonomy: Performance metrics for climate-conscious urban design." Building and environment, 155, (May 2019): 145-160 © 2019 The Author(s)

As Published: 10.1016/j.buildenv.2019.03.028

Publisher: Elsevier BV

Persistent URL: https://hdl.handle.net/1721.1/126763

Version: Author's final manuscript: final author's manuscript post peer review, without publisher's formatting or copy editing

Outdoor Thermal Comfort Autonomy: Performance Metrics for Climate-Conscious Urban Design

Negin Nazarian*[1,2], Juan A. Acero[2], and Leslie Norford[3]

[1]University of New South Wales, Sydney, Australia
[2]Singapore-MIT Alliance for Research and Technology, Singapore
[3]Department of Architecture, Massachusetts Institute of Technology, USA

March 22, 2019

Abstract

Thermal comfort in the built environment is a crucial factor impacting health, well-being, and productivity of urban dwellers. Accordingly, comprehensive analyses are needed to ensure that acceptable criteria of thermal comfort are defined and met in urban environments. The main objective of this study is to define such performance metrics and quality measures of outdoor thermal comfort (OTC), aiming to inform climate-conscious urban design. This article first discusses the motivations for introducing comprehensive thermal comfort metrics, addressing the shortcomings of conventional OTC evaluations that neglect the temporal or spatial variability of OTC. It then introduces four performance metrics, which collectively inform urban planners and designers on the performance of outdoor space with regards to thermal comfort. These metrics build upon the concept of "autonomy" previously introduced for indoor spaces and are extended to include the unique characteristics of outdoor thermal comfort. Second, we discuss the capability of these metrics given the limitations of modeling tools available for urban microclimate analysis, and evaluate the critical factors for an accurate evaluation of Outdoor Thermal Comfort Autonomy (OTCA). We observe that the spatial distribution of airflow at the pedestrian height is critical for OTCA calculation, while the consideration of realistic surface heating depends on the urban density. Lastly, we present an example of employing weather clustering methods such that OTC performance metrics are achieved on an annual basis in a comprehensive yet efficient way. By discussing the capability and the limitations of these metrics we aim to promote climate-conscious design using metrics that are tangible and accessible to non-simulation experts.

Keywords– Outdoor thermal comfort, performance metrics, comfort autonomy, urban design, climate-conscious solutions

1 Introduction

Urban livability, a sum of elements that contribute to the quality of life in cities, is greatly impacted by environmental factors such as water quality, air quality, and climate. Among these, the consideration of

*Corresponding author. Email: n.nazarian@unsw.edu.au. Address: UNSW Built Environment, Room 2023, Level 2, Red Centre West Wing (H13), UNSW Sydney, NSW 2052 Australia. Tel: +61 411 199 096.

thermal comfort is gaining top priority as it directly impacts productivity and cognitive performance [65], well-being, and health of urban dwellers. Additionally, given the increased frequency and duration of extreme heat events [42], such considerations move beyond the prevention of "discomfort" and shift into concerns regarding "stress". Heat stress during extreme weather events is a grave health concern in cities, as mortality is strongly associated with temperature metrics during heatwaves [5, 26, 62], specifically targeting the aging and vulnerable populations with health hazards that are hard to quantify. In summer 2015 alone, over 11,000 people were hospitalized due to hot weather in Japan, with greater concentrations in such urbanized regions as the Greater Tokyo Area [61], while a heat wave in southern India led to over 1,500 deaths [49]. Such global concerns regarding thermal comfort and heat stress call for comprehensive and accurate analyses, aiming to predict and reduce the adverse effects of heat events in future cities and further enhancing city livability.

Although of high importance, Outdoor thermal comfort (OTC) is a notoriously difficult microclimate parameter to evaluate [20, 24, 50, 60], as it involves a combination of various environmental factors, the physiological thermoregulation mechanisms of the human body, and subjective psychological perceptions as well as cultural and climatic backgrounds [8, 20]. Therefore, although thermal comfort is regarded as a critical factor in affecting human health in urban areas, our understanding of OTC compared to other microclimate parameters (such as urban airflow and air temperature) is rather limited. The early studies of thermal comfort involved evaluating indoor spaces [11, 12, 38] and widely assumed that indoor thermal comfort theory generalizes to outdoor settings [55]. However, compared to indoor spaces, there is a lack of thermal boundary in the outdoor environments, exposure to the direct radiation is intensified, and high variability of wind speed is observed. These factors result in great deviations from the thermal comfort neutrality, which further leads to heat stress and makes the thermal comfort analysis intricate. Additionally, due to the predominantly transient behavior of pedestrians in outdoor environments and a vast range of use for outdoor spaces, the physiological and psychological states of each individual become increasingly more complex and important. To address such complexities, the detailed analyses in outdoor urban environments from various perspectives have been proposed [2, 10, 29, 32, 55] and the body of knowledge has grown immensely over the last two decades, contributing to our understanding of outdoor thermal comfort. Using various methods ranging from experimental measurements, survey campaigns, and numerical evaluations, we have learned that:

(a) urban form, size, and configuration have significant effects on outdoor thermal comfort [2, 3, 22, 23, 57, 59];

(b) urban vegetation and trees can mitigate thermal stress in hot climates through modifying radiative and evaporative cooling, although the pedestrian-level wind speed is reduced [3, 31, 41, 52, 58];

(c) the microscale variation in urban heating is significantly important in determining the local effects of comfort and health, and therefore the spatial distribution of thermal comfort, i.e. the location of cold and hot spots, should not be neglected for evaluating thermal stress [22, 34];

(d) regulatory physiological processes of individuals can affect the relative importance of meteorological parameters, which makes thermal comfort variable for different individuals [19, 60]; and lastly,

(e) purely physiological or environmental approaches are not fully equipped for characterizing comfort conditions outdoors, and an understanding of the dynamic "human parameter" (including the psycho-

logical states, cultural and climatic backgrounds, activities, and expectations) is necessary in designing spaces for public use [8, 39].

In addition to addressing the fundamental and pivotal research questions regarding OTC, there has been a quest for defining the most suitable metric that describes the multi-faceted characteristics of thermal comfort. Accordingly, several indices are defined and implemented. The most common indices used for outdoor spaces include: the index of thermal stress (ITS), which represents the ratio between the rate of sweat necessary to maintain the thermal equilibrium to the cooling efficiency of the body based on the microclimate and clothing characteristics[16]; the predicted mean vote (PMV) based on the Fanger comfort model [13], which is an empirical index applicable for field measurements of thermal comfort or indoor analysis; physiologically equivalent temperature (PET), which is "the air temperature at which, in a typical indoor setting (without wind and solar radiation), the heat budget of the human body is balanced with the same core and skin temperature as under the complex outdoor conditions to be assessed" [19]; Standard Effective Temperature (SET), which is an outdoor adaptation of an indoor index based on the effective temperature [15] by considering the mean radiant temperature [45], and Universal Thermal Climate Index (UTCI) based on the multi-node dynamic thermo-physiological UTCI-Fiala model [14] that defines thermal effects on the whole human body.

While thermal comfort indices vary significantly based on the studied parameters and their level of detail, they all aim to comprehensively describe thermal comfort in terms of the contributing factors, and have been widely used to report OTC for various time of the day, different locations, and specific target groups. However, regardless of the thermal comfort metric used, comprehensive "quality measures" for urban design performance with respect to outdoor thermal comfort have not yet been discussed. What are the acceptable or desirable OTC criteria for a given site or a proposed design? And how do people respond to an undesirable OTC? The answer indeed depends on the specific characteristics of each site and requires vigorous research investment to address the "human factor".

In indoor building design, a range of performance metrics exists that can be very specific to a parameter of interest (such as acoustics or daylighting) or general in evaluating the building performance (including sustainability or green measures). For instance, the concept of "autonomy" has been used, which indicates the ability of a space in using passive and available environmental or design resources as opposed to providing active measures for achieving desirable conditions. Specific examples include Daylight Autonomy, which was introduced by Reinhart et al. [47] and has been widely used for assessing the illumination in an indoor design on an annual basis, and Visual Comfort Autonomy [25] which relates the visual comfort of occupants to daylight glare and light adequacy. For the assessment of thermal comfort, a few studies have also discussed performance metrics for indoor environments. Thermal Autonomy was introduced by Levitt et al. [30] such that thermal comfort and energy consumption of buildings are assessed from the architectural perspectives and not the mechanical systems, and Zomorodian and Tahsildoost [66] assessed the effects of window properties in classrooms by employing long-term spatial comfort metrics. Carlucci and Pagliano [7] further reviewed the indices for the long-term evaluation of the general thermal comfort conditions in buildings, and concluded that all the current indices are mainly "single values, i.e. representing one single numerical value summarizing the variety of comfort conditions over certain period of time", and therefore neglecting the spatial variability of thermal comfort in the built environment that is needed for informing

urban design. For outdoor spaces, all together, such performance metrics are lacking. Regarding OTC, while there are detailed description of the strengths and shortcomings of each thermal comfort index at various times and locations, it appears that there are limited efforts on prescribing the collective information that should be delivered to the architects, planners, and decision makers, such that the performance of an outdoor space with regards to thermal comfort is fully assessed.

This gap in the literature motivates the present study. We aim to introduce and define performance metrics that capture the site-specific and dynamic interaction between buildings and the surrounding climate on an annual basis. To do so, we identify the following characteristics that, regardless of the index used for describing the OTC, should be included in any analysis before it can effectively assess and inform the urban design strategies:

(a) consideration of the **temporal variabilities**: yearly analysis of thermal comfort with (sub)hourly resolution for the occupied hours,

(b) consideration of the **spatial variabilities**: spatial distribution of thermal comfort that identifies the "hot/cold spots" and indicates zones of persistent thermal discomfort,

(c) determination of **performance**: percentage of time that an outdoor space meets the desired thermal comfort range, and

(d) determination of **heat stress**: extent of deviation from the desired thermal comfort range that specifies the thermal stress.

Here, we aim to define performance metrics for OTC that consider these characteristics in a comprehensive way, such that they can then be used for comparative studies to guide urban design or to deepen our understanding on OTC in various meteorological conditions.

Figure 1 graphically overviews the present study, identifying the following objectives: 1. defining performance metrics (such as Outdoor Thermal Comfort Autonomy) that cover the holistic characteristic of outdoor thermal comfort (Sec. 2), 2. demonstrating the calculation of performance metrics using a numerical three-dimensional model of OTC and discussing the critical factors contributing to the accuracy of these metrics (Sec. 3), and 3. demonstrating a methodology of utilizing such performance metrics for obtaining a comprehensive yet efficient evaluation of OTC using weather clustering methods (Sec. 4).

2 Performance Metrics for Climate-Conscious Urban Design

This section describes the performance metrics for evaluating OTC in urban design, such that a) they represent comprehensive information in terms of the consideration of temporal and spatial variation of OTC, b) are easily comprehensible and applicable (described in terms of temperature and percentage metrics), and c) represent such critical factors as thermal stress that are relevant to OTC.

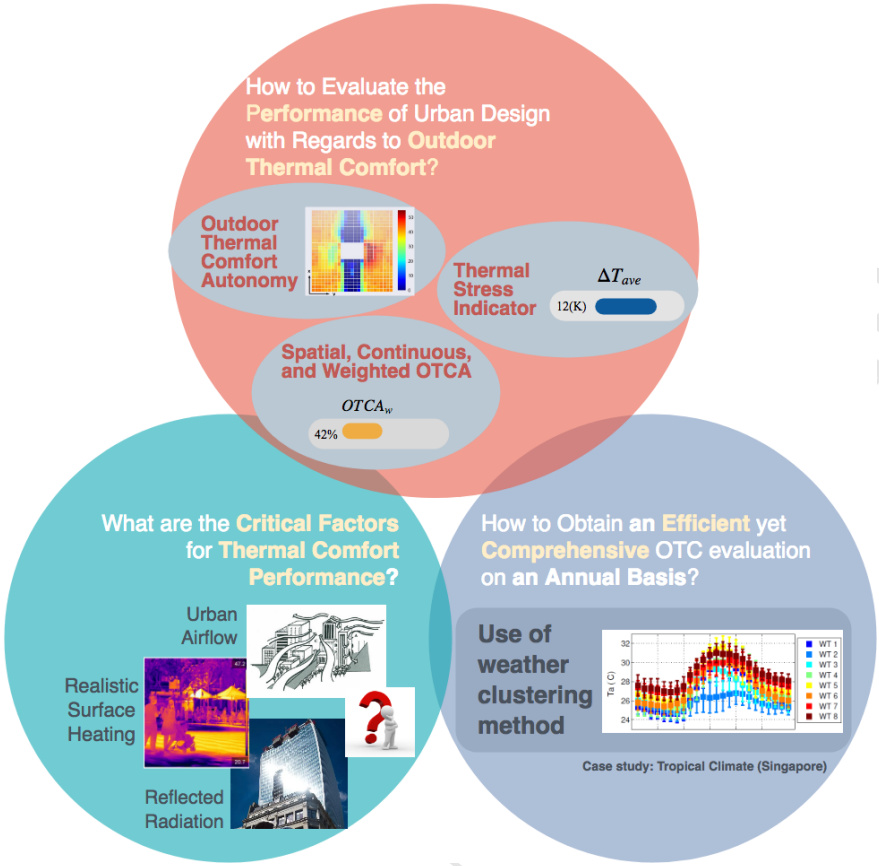

Figure 1: Graphical abstract of the present study indicating the objectives and research questions to be addressed.

2.1 Outdoor Thermal Comfort Autonomy (OTCA)

Outdoor thermal comfort autonomy is defined as the capability of keeping an outdoor space within a prescribed thermal comfort range, without additional cooling equipment or shading devices. Accordingly, ***OTCA*** *is the percentage of occupied time over a year, or a prescribed period of use, where a designated area meets a given set of thermal comfort acceptability criteria.*

The calculation of OTCA is based on a time series of the prescribed thermal comfort metric within the outdoor space. In the current study, Standard Effective Temperature (SET) by Gagge et al. [15] is considered as the evaluation metric, but the presented definition of OTCA can be similarly extended to other thermal comfort indices:

$$OTCA = \frac{1}{N}\frac{1}{n}\sum_{k=1}^{N}\sum_{hr=h_i}^{h_f} TC_{k,hr} \tag{1}$$

$$TC_{k,hr} = \begin{cases} 1 & \text{if SET} \in A \\ 0 & \text{otherwise} \end{cases} \tag{2}$$

where $TC_{k,hr}$ is the thermal comfort index at a given day and hour, A is the "thermal comfort acceptability criteria," i.e. the thermal comfort range that describes the desirable OTC conditions at a specific outdoor

space, N is the total number of occupied days, h_i and h_f denote the initial and final hours of occupation per day, and n is the total occupied hours ($n = h_f - h_i$). Here, $TC_{k,hr}$ is considered as either thermal comfort index calculated at hourly intervals or the time-averaged value over an hour of study.

An example of an OTCA map at the pedestrian height (1.5m) is demonstrated in Fig. 2 for an idealized array of buildings (a matrix of 3×3 equally spaced cubes with uniform height and plan area density, λ_p, of 0.0625). In this example, the operational hours are set to 0900 (h_i) to 1800 (h_f) local time while the acceptable OTC range (A) is set to 20-28°C. The large spatial variability seen in the OTCA map is attributed to the spatial distribution of wind speed (Fig. 2-b) as well as the cumulative effects of the shading pattern during the operational hours. Accordingly, the OTCA in adjacent grid cells may significantly differ, reflecting the combined impact of wind speed and shading on thermal comfort.

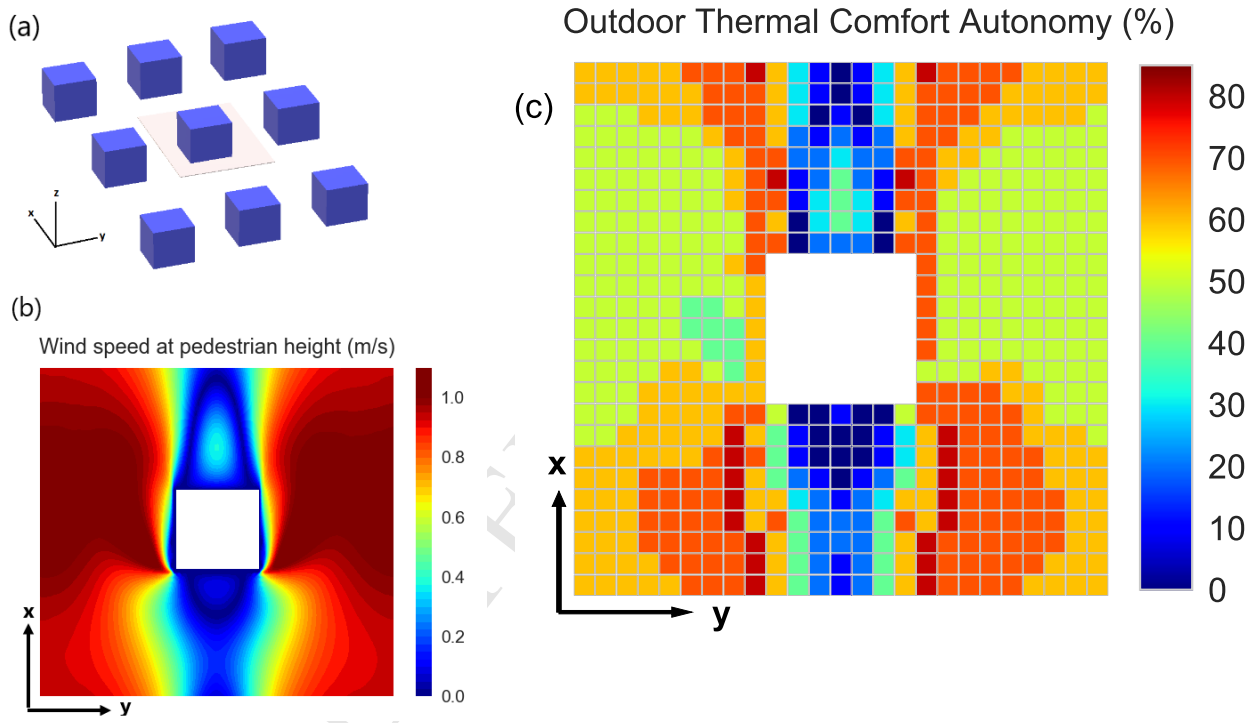

Figure 2: a) Schematic of a 3D array of idealized buildings with $\lambda_p = 0.0625$, b) spatial distribution of wind speed at the pedestrian height (1.5m) obtained from CFD [35], and c) an example of the spatial distribution of OTCA calculated at the pedestrian height (1.5m) for the configuration shown in (a). The example shown here is calculated for a typical dry-season day in Singapore during the month of March (meteorological data further discussed in Sec. 4.1.1 and Appendix B). The sun path during the studied day is from East to West at the equinox.

It is important to note that the calculation of OTCA requires the detailed consideration of human behaviors within the scope of the studied outdoor space as well as the expectation of the thermal environment. For example, the occupied hours, n, would be different based on the use of an outdoor space and should be factored in here for an accurate analysis of OTC. Additionally, the "acceptable" thermal comfort range in outdoor spaces is often larger than in indoor spaces, and varies based on the use of the outdoor space and the expectations of occupants. A recent study by Yang et al. [64] showed that the range of acceptable operative

temperature in outdoor urban spaces in Singapore can go as high as 31.7 $^{\circ}C$, which is significantly larger than the prescribed neutral range. Additionally, comparing the surveys carried out in semi-outdoor food-courts [54] with outdoor areas in Singapore [64], it can also be seen that the preferred temperature range can change up to 1.5$^{\circ}C$ in the same city, solely based on the functionality of a space. Such variations are more significant across different cities. Chow and Heng [9] has compared the neutral PET range for 10 major cities around the globe, and demonstrated that the reported range for "neutral comfort" can range from 18°C (Glasgow, UK [28]) to 29°C (Rome, Italy [51]), and the review of numerous studies by Potchter et al. [46] revealed that the range of the thermal comfort or dis-comfort varies strongly between hot and cold climates. Such variations are attributed to the acclimatization of the occupants to the local climate, their expectation of an outdoor space and climatic backgrounds, and physiological conditions of participants, which further call for the calibration of the thermal comfort acceptability criteria (A in Eq. 1) for the accurate calculation of OTCA.

2.2 Spatial and Continuous OTCA

*The **Spatial OTCA** is defined as the percentage of an outdoor space that is within the desired thermal comfort range at least 50% of the occupied time (over a year or a prescribed period of use).*

Additionally, partial credit can be attributed when thermal comfort lies below the threshold. Accordingly, ***Continuous OTCA*** *extends the definition of Spatial OTCA such that partial credit is given in an outdoor space where OTCA is lower than 50% threshold.*

For example, in the space where the OTCA is 40%, Continuous OTCA considers a partial credit of 40/50=0.8. In the example shown in Fig 2, the Spatial OTCA is **7%**, while Continuous OTCA is calculated as **13.4%**. The concepts of spatial and continuous OTCA are analogous to spatial and continuous daylight autonomy introduced by Reinhart et al. [47] as annual daylight metrics for indoor building design, and are defined to present and compare the performance of an outdoor space with regards to OTC in a tangible manner.

The spatial distribution of OTCA (shown in Fig. 2) is important in identifying the location of persistent "cold" or "hot" spots in urban areas, while Spatial and Continuous OTCA assess the overall performance of an outdoor space. There are valid arguments for considering both the spatial distribution of OTCA (Fig. 2) or the spatially-averaged quantities such as Spatial and Continuous OTCA as a design metric. As thermal comfort is highly variable in an outdoor space, the information provided in the spatial map of OTCA identifies the locations that are consistently outside of the thermal comfort acceptability criteria, and therefore urges designers to use passive design elements (such as shading devices) or active cooling methods (such as fans) for improving thermal comfort in these locations. However, pedestrians are often mobile in an outdoor urban space and at any time can move to a neighboring location with a desired thermal comfort range. This adaptive thermal comfort behavior should be considered in urban design, as it may not be needed nor feasible to design a space for 100% spatial autonomy. Therefore, Spatial and Continuous OTCA can be used as an adaptive and averaged thermal comfort evaluation.

Lastly, the threshold 50% here is considered analogous to the daylight autonomy, but more importantly, due to the fact that in outdoor urban spaces, people are often mobile and not bound to fixed position (contrary to the case indoor). However, we note that this threshold highly depends on the functionality of the outdoor

space. For instance, in case of alfresco outdoor dining, it is more suitable to pick a higher threshold such as 80%, while in case of recreational outdoor space, park areas, or areas where people can move to chose their location in the urban area, the %50 is deemed acceptable.

2.3 Thermal Stress Indicator: Deviation from the Thermal Comfort Acceptability Criteria

*The **Thermal Stress Indicator** is defined as the average deviation of the thermal comfort index from the acceptable OTC range in an outdoor space, calculated during the occupied time over a year or a prescribed period of use.*

When calculating the outdoor thermal comfort autonomy, the OTC index is computed and discarded if not within the acceptability criteria. Accordingly, the computation of OTCA can be regarded as "binary" with no indication of the magnitude of deviation from the acceptable range, and therefore neglecting the extent of thermal stress. To give more information on OTC, the Thermal Stress Indicator can be computed as the average deviation of temperature from the desired range at each location:

$$\Delta T_{ave} = (K^{-1} - 1)\Delta T_{crit} \tag{3}$$

where K, the scaling factor between 0 to 1, is computed as

$$K = \frac{1}{N}\frac{1}{n}\sum_{k=1}^{N}\sum_{hr=h_i}^{h_f} m_{k,hr} \tag{4}$$

$$m_{k,hr} = \begin{cases} 1 & \text{if } \mid \Delta T \mid \leq \Delta T_{crit} \\ \frac{\Delta T_{crit}}{|\Delta T_{k,hr}|} & \text{otherwise} \end{cases} \tag{5}$$

Here, ΔT_{crit} is the acceptable temperature range from the midpoint, defined as

$$\Delta T_{crit} = (A_{max} - A_{min})/2. \tag{6}$$

For instance, if the thermal comfort acceptability range (A in Eq. 1) is set to 20 - 28°C, then $\Delta T_{crit} = 4°C$. $\Delta T_{k,hr}$ is then defined as the difference of the thermal comfort index at any time and day ($TC_{k,hr}$) from the midpoint of the acceptable range A, calculated as

$$\Delta T_{k,hr} = TC_{k,hr} - (A_{max} + A_{min})/2. \tag{7}$$

Accordingly, ΔT_{ave} (Eq. 3) at every location indicates the (absolute) average deviation (in °C) of the thermal comfort index from the acceptable OTC range during the occupied time over a year, and therefore identifying the zones with critical thermal stress conditions throughout the occupied time (Fig. 3).

It is worth noting that the definition of scaling factor described in Eq. 4 a) neglects the distinction between "hot" and "cold" spots and solely considers the absolute value of temperature deviation, and b) does not indicate the frequency of occurrence of events within the thermal stress zone (i.e. 10 slightly uncomfortable days may result in a similar K factor than 1 extremely uncomfortable day out of 10 days). Therefore, for obtaining more information and presenting a comprehensive assessment, it is suggested to divide this metric

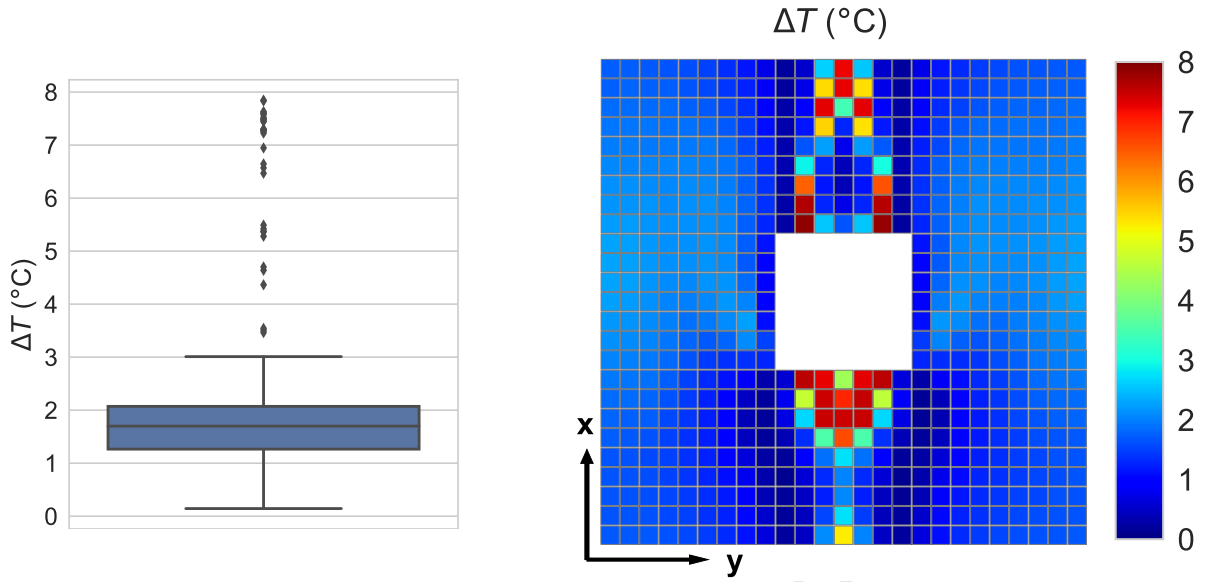

Figure 3: The spatial distribution (right) and box-and-whisker diagram (left) of ΔT_{ave} as the Thermal Stress Indicator (Eq. 3) calculated at the pedestrian level for an idealized array of building ($\lambda_p = 0.0625$). The example shown here is calculated for the same case and configuration discussed in Fig. 2 and Sec. 2.1.

into different bands (hot and cold) by considering K^+ and K^- based on the sign of $\Delta T_{k,hr}$. Additionally, the frequency of deviation in the cold and hot bands can be calculated in order to add more information regarding the occurrence of thermally uncomfortable conditions:

$$f_i = \frac{1}{N}\frac{1}{n}\sum_{k=1}^{N}\sum_{hr=h_i}^{h_f} F_i \quad \text{where i= \{cold, OK, hot\}} \tag{8}$$

$$\text{Cases}= \begin{cases} F_{cold} = 1 & \text{if } \mid \Delta T_{k,hr} \mid > \Delta T_{crit} \wedge \Delta T_{k,hr} < 0 \\ F_{OK} = 1 & \text{if } \mid \Delta T_{k,hr} \mid \leq \Delta T_{crit} \\ F_{hot} = 1 & \text{if } \mid \Delta T_{k,hr} \mid > \Delta T_{crit} \wedge \Delta T_{k,hr} > 0 \end{cases} \tag{9}$$

Following these calculations, the spatial map of ΔT_{ave} as a Thermal Stress Indicator (Fig. 3) together with the spatial map of frequency of occurrence (Eq. 8) can provide comprehensive information which distinguishes the persistent occurrence of "hot" and "cold" conditions from a potentially short-lived extreme event.

2.4 Weighted Outdoor Thermal Comfort Autonomy ($\boldsymbol{OTCA_w}$)

Here, we introduce the **Weighted Outdoor Thermal Comfort Autonomy** ($OTCA_w$) to represent the average deviation from the acceptable OTC range together with the OTCA map, as opposed to considering the binary approach to comfort previously discussed in Eq. 1. Accordingly, ***$OTCA_w$*** *represents the percent of occupied time over a year, or a prescribed period of use, where a thermal zone meets a given set of thermal comfort acceptability criteria, while also accounting for the deviation (thermal stress) when the desired OTC range is not met.*

Using the scaling factor K (Eq. 4), OTCA can further be weighted to include the deviation of the thermal comfort index from the acceptable OTC range during the occupied time over a year, such that

$$OTCA_w = K \times OTCA. \tag{10}$$

Figure 4 demonstrates the variability in OTCA compared with OTCA_w and indicates the importance of including the deviation from the acceptability criteria.

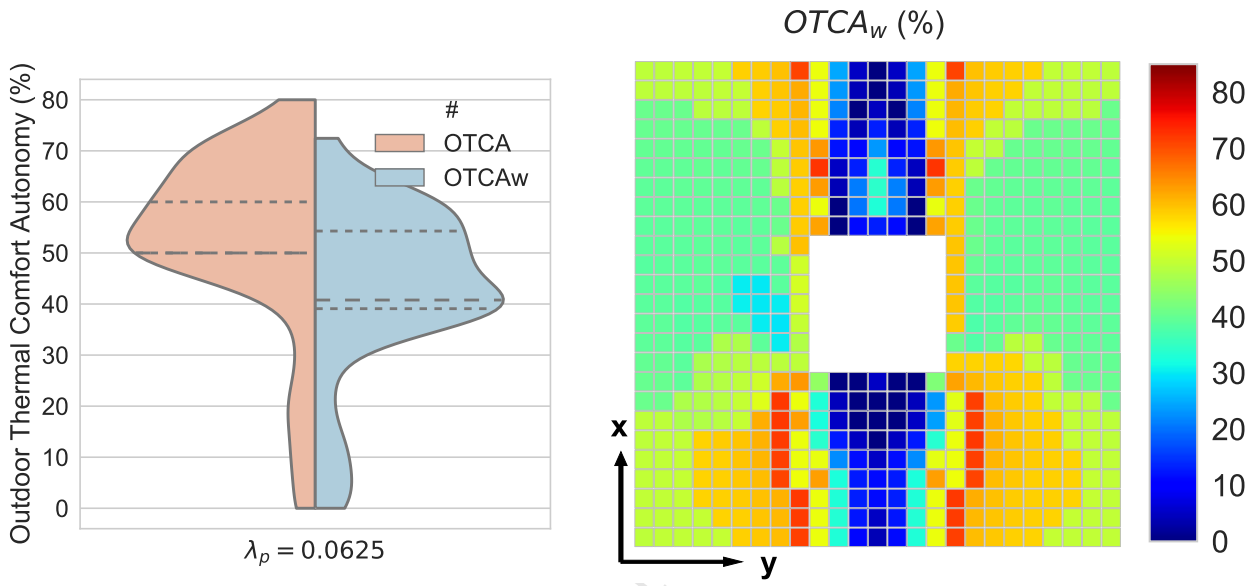

Figure 4: Spatial distribution of OTCA_w (right) and violin plot (kernel density) distribution of OTCA and OTCA_w (left) at the pedestrian height for an idealized array of building ($\lambda_p = 0.0625$). The example shown here is calculated for the same case and configuration discussed in Fig. 2 and Sec. 2.1. The inner lines in the violin plots demonstrate the quartiles of the distribution.

3 Critical Factors for Thermal Comfort Performance

Subsequent to defining the performance metrics for thermal comfort, it is paramount to discuss the means for their accurate estimation. Here, we present a series of sensitivity analyses which evaluate the role of various microclimate parameters in the OTC performance. This analysis is motivated by the state-of-the-art numerical models currently used for assessing OTC and the assumptions and limitations associated with them. The goal is to draw attention to the ways in which such assumptions can impact an accurate evaluation of thermal comfort in urban spaces, quantified by OTC performance metrics such as OTCA (Sec. 2). Although it is out of the scope of the present study to conduct a comprehensive set of sensitivity analyses, the discussion given in this section is critical in presenting a comprehensive perspective regarding the OTC performance metrics and aim to emphasize on accurate assessments using numerical models. Overall, three critical parameters are examined:

(a) **Spatial distribution of urban airflow**: we consider the assumption of uniform wind speed at the pedestrian level as opposed to obtaining the detailed three-dimensional distribution of airflow (often

obtained from Computational Fluid Dynamics simulations).

(b) **Realistic distribution of surface heating**: the non-uniform three-dimensional distribution of surface temperature, and the subsequent role on the spatial distribution of OTCA, is examined compared to the assumption of uniform surface temperature for urban facades.

(c) **Reflected radiation from urban facades to pedestrians**: we evaluate the implications of neglecting the reflected radiation from urban facades on radiation exposure of pedestrians, and consequently, the performance of an outdoor space with regards to thermal comfort.

3.1 Case Studies

The sensitivity analysis presented here is conducted for Singapore (between 1°09′N to 1°29′N, and 103°36′E to 104°25′E). More information on the climatic characteristics of Singapore is given in Sec. 4.1.1. The simulation days correspond to the month of April, which encompasses the highest air temperature and largest solar elevation angle. The test case presented here is an idealized array of buildings, while the plan area density (λ_p) is varied from 0.0625 to 0.44, representing Sparsely Built (LCZ 9) and Compact Mid-Rise (LCZ 2) Local Climate Zones, respectively [56]. Each building wall has a window with window-to-wall ratio of 0.4 and solar heat gain coefficient (SHGC) of 0.2. The albedo and emissivity of urban surfaces (walls and ground) are set to 0.3 and 0.9, respectively. The relative humidity is considered constant at the pedestrian level and set to 80%, which is the annual average of humidity in Singapore.

To obtain the most comprehensive analysis, a modular approach detailed by Nazarian et al. [37] is used such that existing microclimate tools of airflow and energy balance modeling contribute to the calculation of OTC. Accordingly, the surface temperatures and canopy air temperature is obtained from energy balance modeling using the Temperature of Urban Facets Indoor-Outdoor Building Energy Simulator (TUF-IOBES [63] and [27]), while the flow field is taken from large-eddy simulations (LES) of Nazarian et al. [35, 36]. For thermal comfort analysis, SET is taken as the OTC metric and calculated for a standing male pedestrian (metabolic rate = 1.2) who weighs 70 kg, is 150cm tall, and is wearing light summer clothing (iclo=0.34). The skin wetness, body emissivity, and body albedo are considered to be 0.088, 0.95, and 0.3, respectively. The OTC performance metrics are calculated for an outdoor space with operational hours of 0900 (h_i) to 1800 (h_f) local time, while the acceptable OTC range, A in Eq. 1, is set to 20-28°C. This range covers the neutral zone prescribed in SET definition ($22.2 - 25.6°\,C$ Auliciems and Szokolay 1997), as well as mid-range of slightly cold or slightly warm thermal zone, which is found to be acceptable in outdoor dining places in Singapore [64].

Table 1 represents the simulation cases that are studied here. The Base case represents the OTCA calculation with realistic 3D distributions of surface temperature and reflected radiation (taken from TUF-IOBES) and flow field (taken from LES simulations). The detailed description of other simulation cases are provided in the following sections.

Table 1: Proposed Case Studies for OTCA analysis

ID No.	Cases	Boundary Conditions		
		Surface Temperature	Airflow	Reflected Radiation
1	Base	Realistic (3D)	Realistic (3D)	Realistic (3D)
2	Wind-Test	Realistic (3D)	**Constant**	Realistic (3D)
3	Temp-Test	**Constant**	Realistic (3D)	**Constant**
4	Refl-Test	Realistic (3D)	Realistic (3D)	**Neglected**

3.2 On the Consideration of Urban Airflow in Thermal Comfort Autonomy

Here, we calculate the OTCA (Eq. 1) for an idealized array of building with plan area density (λ_p) of 0.0625 (shown in Fig. 5-a), and compare the following assumptions for wind conditions at the pedestrian level:

1. three-dimensional distribution of airflow for the representative urban configuration ($\lambda_p = 0.0625$) obtained using a CFD simulation [35] (Base in Table 1),
2. constant wind speed at all the pedestrian locations: value calculated based on the spatial mean of the airflow at the pedestrian height (Wind-Test in Table 1 with u=0.7 $\mathrm{m\,s^{-2}}$), and
3. constant wind speed at all the pedestrian locations: value based on the hourly-average of wind speed at the reference height above the canopy (Wind-Test in Table 1 with u=2 $\mathrm{m\,s^{-2}}$).

The realistic (3D) distribution of surface temperature and reflected radiation is considered in these cases. Figure 5 demonstrates the distribution of airflow at the pedestrian height (b) as well as the OTCA distribution for the wind conditions considered here (c-d): uniform and realistic distribution of wind speed at the pedestrian height. The spatial distribution of OTCA is significantly different in the two studied cases. When the wind is considered constant at all pedestrian locations, it can be seen that the spatial distribution of OTCA is dominated by the change in the shadow pattern throughout the occupied hours (0900 - 1800 local time). When the spatial distribution of the airflow is introduced, however, the spatial distribution of OTCA is modified to represent the flow field in addition to the shadow patterns, and consequently, the location of the "hot" and "cold" spots is modified.

Figure 6 further displays the violin plot distribution of OTCA in the three studied conditions, and it can be seen that not only the spatial distribution of the wind speed, but also the value assigned at the pedestrian height, has a significant importance in the OTCA outcome. In the case of using a higher above-canopy wind speed ($2\mathrm{m\,s^{-1}}$), the OTCA is generally larger than 50%, yielding a 100% spatial autonomy which is in contrast to the case with wind speed $0.7\mathrm{m\,s^{-1}}$ (taken as the average of the airflow at the pedestrian level) where the spatial OTCA is 0%. Similarly, when spatial distribution of wind speed is considered, the average deviation of the thermal comfort from the acceptable range (i.e. thermal stress indicator discussed in Sec. 2.3) can reach up to $12°C$ in some pedestrian locations (shown in the boxplot of ΔT_{ave} in Fig. 6) due to the formation of vortices before and after the building that significantly reduce the wind speed value. However, this extent of deviation from the acceptable thermal comfort range is not reflected in the cases with constant wind speed. Given these findings, it is evident that the consideration of the detailed flow field in urban environments is critical in evaluating the performance metrics for outdoor thermal comfort.

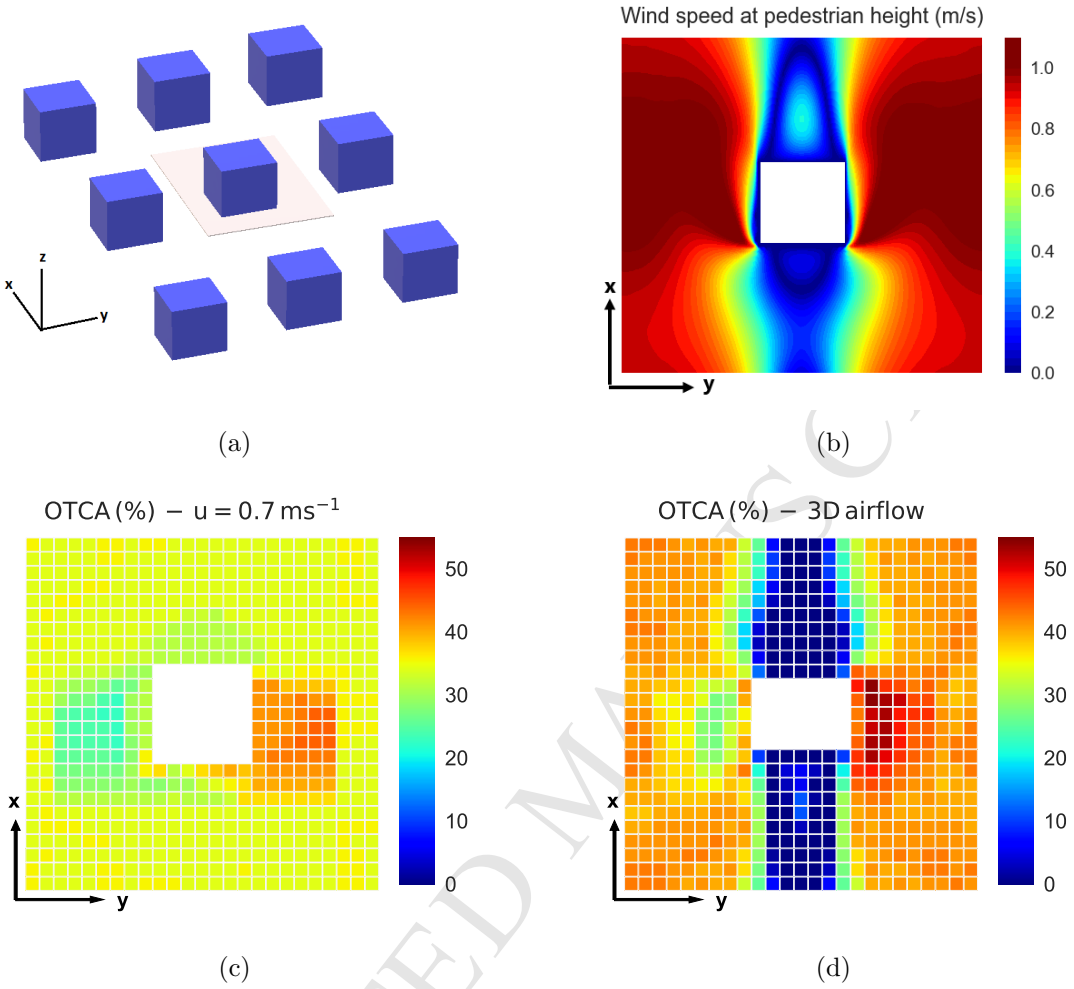

Figure 5: (a) Schematic of the computational domain as an idealized array of buildings, (b) spatial distribution of wind speed at the pedestrian height obtained from CFD [35], and the distribution of OTCA at the pedestrian height (z=1.5m) considering a uniform (0.7 $\mathrm{m\,s^{-1}}$) and realistic wind speed, (c) and (d) respectively.

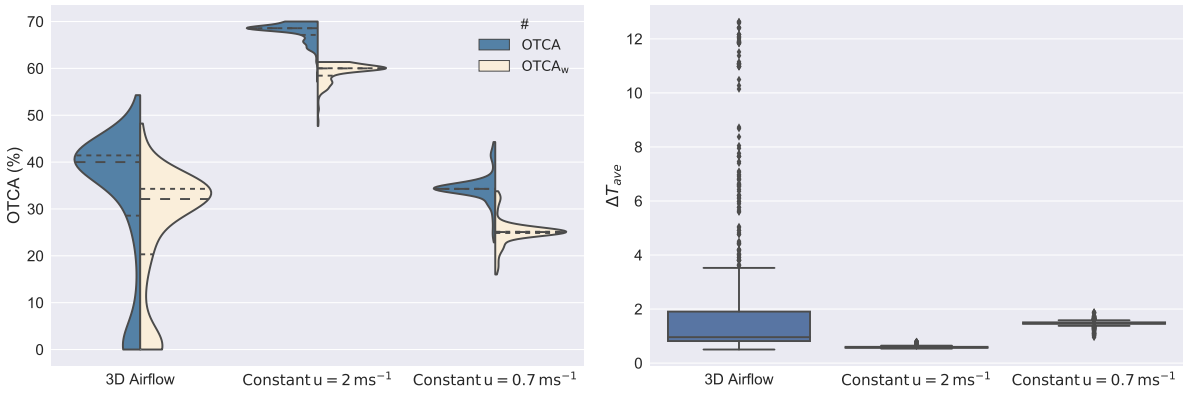

Figure 6: Left: violin plot distributions of OTCA and $\mathrm{OTCA_w}$ (Eqs. 1 and 10) and right: box plots of ΔT (Eq. 3) for $\lambda_p = 0.0625$ at the pedestrian level in 3 different wind conditions.

3.3 On the Consideration of Realistic Surface Heating in Thermal Comfort Autonomy

In this section, we evaluate OTCA calculation using two assumptions made for the temperature of urban facades:

1. non-uniform three-dimensional distribution of surface temperature obtained using a building-to-canopy energy balance model considered at urban facades (Base in Table 1), and
2. uniform (constant) temperatures considered at each surface, taken as the average value of surface temperature (Temp-Test in Table 1).

Figure 7 demonstrates an example of non-uniform surface hearing at the ground level for $\lambda_p = 0.0625$ at 1000 local time, which is strongly dominated by the shading pattern. It is worth noting that the consideration of detailed shading on the pedestrian (and not surfaces) is kept intact here as it dramatically changes the analysis of thermal comfort, and only the distribution of surface temperature is of focus here. Additionally, the spatial (non-uniform) distribution of airflow at the pedestrian height is considered in these cases.

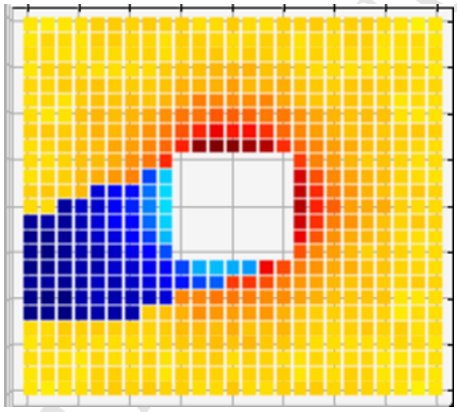

Figure 7: Spatial distribution of ground-level surface temperature at 1000 local time for $\lambda_p = 0.0625$.

We observe that the spatial distribution of OTCA at the pedestrian level is dominated by the spatial distribution of airflow and shading patterns (at pedestrian locations) during the occupied hours (similarly shown in Fig. 5), and therefore the assumption of uniform surface heating did not dramatically impact the OTCA map (not shown). However, the value of OTCA can be slightly impacted as shown in the violin plot in Fig. 8. When the 3D distribution of surface temperature is not considered, the OTCA values are slightly overestimated (up to 3% observed here). However, Nazarian et al. [37] demonstrated that the consideration of realistic surface heating affects the mean radiant temperature at the pedestrian height more significantly in the higher urban densities, which is expected to similarly affect the OTCA distribution. Accordingly, the accurate calculation of OTCA in high-density urban environments requires a careful attention to the surface heating distribution and further investigations are needed to evaluate the variation in OTCA based on urban density and surface properties.

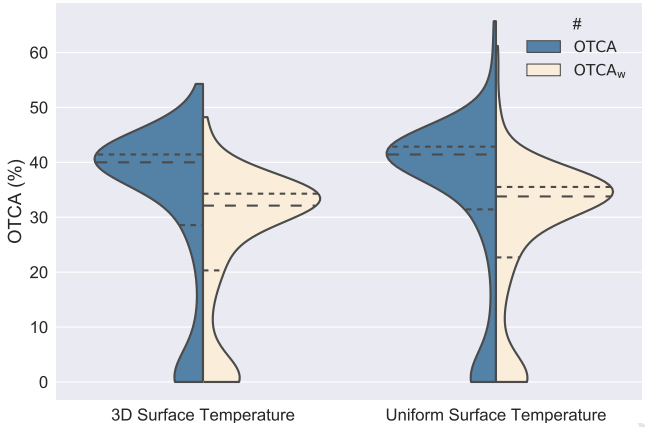

Figure 8: Violin plots of OTCA and OTCA$_w$ (Eqs. 1 and 10) for $\lambda_p = 0.0625$ at the pedestrian level in two different surface heating conditions.

3.4 On the Consideration of Reflected Radiation in Thermal Comfort Autonomy

Lastly, we evaluate the OTCA calculation given the assumption of reflected radiation. In several existing thermal comfort models, the reflected radiation from surfaces that are visible to the pedestrians is neglected while it is expected to have a tangible impact, particularly when pedestrians are exposed to highly-reflective surfaces in densely-built urban areas. To assess this assumption, we evaluate the difference in OTCA distribution for two scenarios: with and without the consideration of reflected radiation in the calculation of OTC. The realistic distribution of wind speed at the pedestrian height and realistic surface heating is maintained for both cases. The analyses are done for two urban densities: 1) $\lambda_p = 0.0625$ representing "sparsely built" Local Climate Zone (LCZ 9) and 2) $\lambda_p = 0.44$ representing "compact mid-rise" Local Climate Zone (LCZ 2).

Figure 9 demonstrates the distribution of OTCA and OTCA$_w$ for two urban configurations with and without reflected radiation from the visible urban surfaces. It can be seen that in both LCZs, neglecting the surface reflected radiation leads to the overestimation of both OTCA and OTCA$_w$. In the $\lambda_p = 0.44$ case, the median OTCA is changed up to 7%, which demonstrate the importance of surface reflected radiation in outdoor thermal comfort. It is worth noting that, here, only one value of surface albedo ($\alpha = 0.3$) is considered and therefore further investigations are needed to evaluate the importance of reflected radiation in OTCA given the variability of surface albedo and considering a full range of local climate zones.

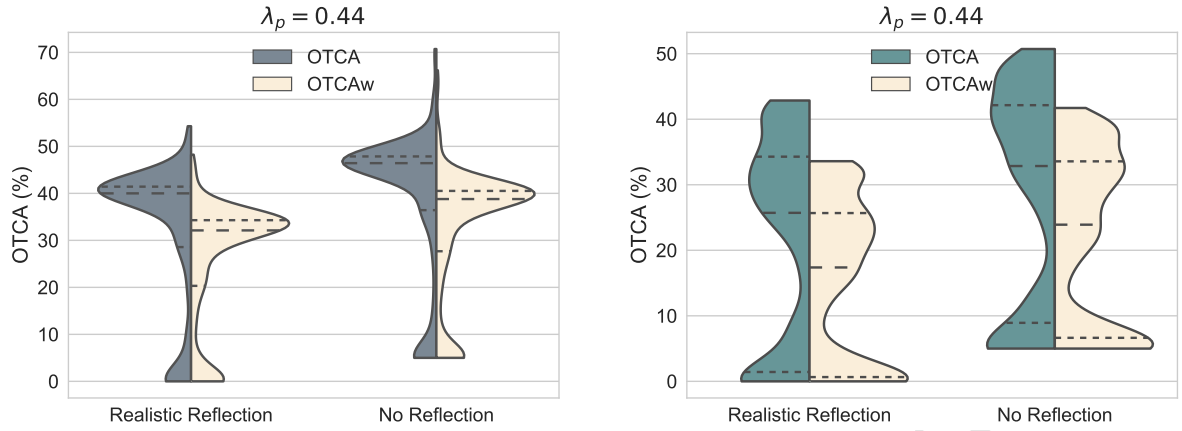

Figure 9: Violin plots of OTCA and OTCA_w (Eqs. 1 and 10) for $\lambda_p = 0.0625$ and $\lambda_p = 0.44$ at the pedestrian level with and without the consideration of reflected radiation.

4 Comprehensive Annual Evaluation of Thermal Comfort Metrics

After discussing the OTC performance metrics and drawing attention to the critical factors that should be scrutinized in their calculation, here we discuss a methodology to obtain a comprehensive yet efficient evaluation of OTC performance metrics. The aim is to minimize the computational costs of calculation while maintaining the variability in meteorological conditions, which is needed for detailed analyses on an annual basis.

In order to fully evaluate and describe the thermal comfort performance in urban design scenarios, it is essential that both spatial distributions (calculation of OTC at various pedestrian locations in urban areas) and temporal variabilities (consideration of hourly meteorological data) are represented. This calculation involves a coupling of several physical models at each hour of calculation, which can impose further limitations and simplifications of the processes. Here, as an alternative method for maintaining the spatial and temporal characteristics, we discuss a clustering method for the input meteorological data that can be utilized for effective calculation of OTC performance metrics.

4.1 Weather Clustering Method

The common method for implementing the meteorological forcing in urban climate simulations is to obtain the long-term databases of atmospheric parameters throughout at least one year, and directly use them in the numerical models. Such datasets are represented as locally recorded weather data or pre-selected "typical" years, which are available with a high temporal frequency (1-3 h). A comprehensive yearly energy and comfort analysis then needs to integrate the hourly representative meteorological forcing data. This approach is common for building or urban energy-balance analyses, where 8760 sets of forcing data (corresponding to yearly data with hourly resolution) are used, but poses several challenges for the comprehensive assessments of thermal comfort that depends on a range of microclimate parameters such as wind speed, air temperature, mean radiant temperature, and humidity. The main challenge arises when the variabilities in

the meteorological forcing are needed in the dynamic coupling of the underlying physical models, such as urban flow field and energy balance models. Due to the complexities of such coupling methods, the hourly variation of all parameters is not commonly considered. The second challenge is computational costs and storage limitations. An annual analysis takes up a significantly large CPU and storage capacity. As a result, the consideration of all hours for an annual analysis may not be feasible, and perhaps is unnecessary.

To address such challenges to the comprehensive annual analysis of thermal comfort, a method to cluster the yearly meteorological data has been proposed. The goal of clustering is to obtain the representative weather types that describe the typical daily patterns, and further produce synthetic long-term climatic forcing in an efficient way. Previously, this approach was mostly implemented for the synoptic-scale circulation analysis [21, 44], but a recent study by Acero et al. [1] has demonstrated that the application of weather clustering can be extended to microscale climate simulations.

The process of weather clustering is as follows. Site observations are identified for a sufficiently long period that represents the diversity of weather types throughout the year and a clustering method is applied to classify the meteorological conditions of each day (a detailed description of the clustering method employed here is explained in Appendix A and Acero et al. [1]). In each cluster, a diurnal cycle is then calculated for each climate variable. As a result, sequences of weather data are reconstructed at an hourly frequency for all forcing variables such that they represent the climatic variability of a location in terms of wind regimes, precipitation, thermal range, and humidity amplitude for an entire year. Previous studies, such as Hidalgo et al. [17], have shown that such reconstruction algorithms are able to produce diurnal cycles that compare well within the hourly series from observations. Similarly, in order to achieve a comprehensive yet efficient analysis of OTC performance metrics, we propose and evaluate a weather clustering method here. The following sections describe an example of such analysis for a tropical climate of Singapore.

4.1.1 Example of Clustered Weather Data in a Tropical Climate of Singapore

This section details an example of clustered weather data for a case study of Singapore. Singapore is an island state located in Southeast Asia (between 1°09′N to 1°29′N, and 103°36′E to 104°25′E) and its climate is characterized by uniform air temperature and high humidity throughout the year with small diurnal and seasonal variations. Accordingly, the minimum and maximum air temperature range between 23-25°C and 31-33°C, respectively, while the relative humidity (in the absence of rain) varies from 60% in the afternoon to 90% in the morning (before sunrise). In the rainy periods, however, the RH reaches 100%, resulting in an annual average of 84%. Further contrasts that prevent true all-year uniformity are the monsoon seasons occurring twice a year. These monsoon seasons, labeled as Northeast (NE) and Southeast (SE) monsoons, are characterized by increased precipitation and prevailing wind directions, and the highest precipitation levels usually occur during the wet Northeast monsoon season [33, 48].

In order to obtain the clustered weather data for Singapore, the EnergyPlus Weather data (EPW file extension retrieved from https://energyplus.net/weather) was used, which includes an hourly dataset of a typical year. This data represents compiled observations from multiple years collected at the Singapore Changi Airport meteorological station. The following variables are then chosen to cluster the yearly meteorological data into "typical" days using the statistical clustering K-Means method (Appendix A):

- Daily mean air temperature, T_a ($^\circ C$)
- Daily temperature amplitude, dT ($^\circ C$).
- Daily mean vapour pressure, e_v (Pa)
- Daily mean global horizontal irradiance, GHI ($\mathrm{W\,m^{-2}}$)
- Daily mean wind speed and direction, WS and WD ($\mathrm{m\,s^{-1}}$ and $^\circ$)

Table 2 summarizes the eight weather types (clusters) obtained for Singapore using the prescribed method. The clustered weather types where obtained from the entire year, as opposed to separating the meteorological data into various climatic periods (e.g. monsoons, and inter-monsoon seasons). This is acceptable due to the low inter-seasonal variability of climate in Singapore, but may not be recommended in the temperature climates and other locations with distinct seasonable variability [18].

Table 2: Summary of the typical weather types in Singapore obtained by the clustering method. The four possible **Seasons** for each clusters are 1) Northeast (NE) Monsoon season (December - early March), 2) Inter-Monsoon period (late March - May), 3) Southwest (SW) Monsoon season (June - September), and 4) Inter-Monsoon period (October - November). **WD** and **WS** stand for wind direction and wind speed, respectively, and **Rain** indicates the expected precipitation level. The columns **Months** and **Date** represent the months of occurrence for each cluster and the selected date of simulation corresponding to that period, respectively. f is then the frequency of occurrence for each weather type.

ID	**Season**	**WD**	**WS**	**Rain**	**Months**	**Date**	f
1	NE monsoon, Dry	NE	Medium-High	None-Low	Feb, Mar	1-Mar	11.8%
2	NE monsoon, Wet	NE	Low	High	Dec, Jan	1-Jan	10.4%
3	Inter-monsoon, Wet	-	Low	Medium	Oct, Nov	1-Nov	20.0%
4	SW monsoon	SW	Medium	Low	Aug, Sep	1-Sep	11.5%
5	NE monsoon, Dry	NE	Low-Medium	Low	Feb, Mar, Apr	15-Mar	16.7%
6	NE monsoon, Dry	NE	High	None-Low	Feb, Mar	1-Mar	8.0%
7	SW monsoon, Inter-monsoon	S-SE	Medium	None-Low	Apr - Sep	1-Jul	11.2%
8	SW monsoon	SW	Medium	low	May-Sep	15-Jul	10.4%

Further description of the characteristics of each clustered weather type is presented in Appendix B. Overall, the mean hourly values and the diurnal amplitude are well represented, especially for variables with pronounced diurnal variations such as incoming solar radiation, temperature, and humidity. The variability in wind flow is also represented reasonably well but with lower value of Pearson correlation coefficient than other parameters, which has been similarly reported in Hidalgo et al. [17]. Accordingly, although the clustering method represents the daily variability in some climatic variables better than others (Appendix B Table B.1), it can be concluded that the overall weather types obtained here are reliable for a yearly thermal comfort analysis. The forcing data in each weather type (including air temperature, relative humidity, wind speed and direction, short-wave radiation (DNI, GHI, DHI), cloud cover, and ceiling height) are then used for the calculation of OTC performance metrics detailed in the following section.

4.2 Calculation of OTC Performance Metrics using the Clustered Weather Data

Here, the clustered weather types obtained for Singapore (summarized in Table 2) are used to demonstrate the comprehensive calculation of OTC performance metrics for an entire year. Figure 10 displays the flowchart of the presented methodology. In order to obtain a more comprehensive analysis, we employ a modular approach such that existing microclimate tools for urban energy balance and airflow modeling provide the microclimate inputs needed for calculating thermal comfort [37]. First, instead of using the hourly values of meteorological data for an entire year, the clustered weather types (detailed in Sec. 4.1.1) are considered. Then, for each weather type, the energy balance simulations are run and the 3D distribution of surface temperature and radiation are obtained. Next, these results are combined with the airflow at the pedestrian level, simulated using Computational Fluid Dynamics (CFD) modeling, and the 3D distribution of the thermal comfort index is calculated. Lastly, the performance metrics are obtained for each weather type and weighted based on the frequency of each type (Table 2) to calculate the annual OTC performance metrics.

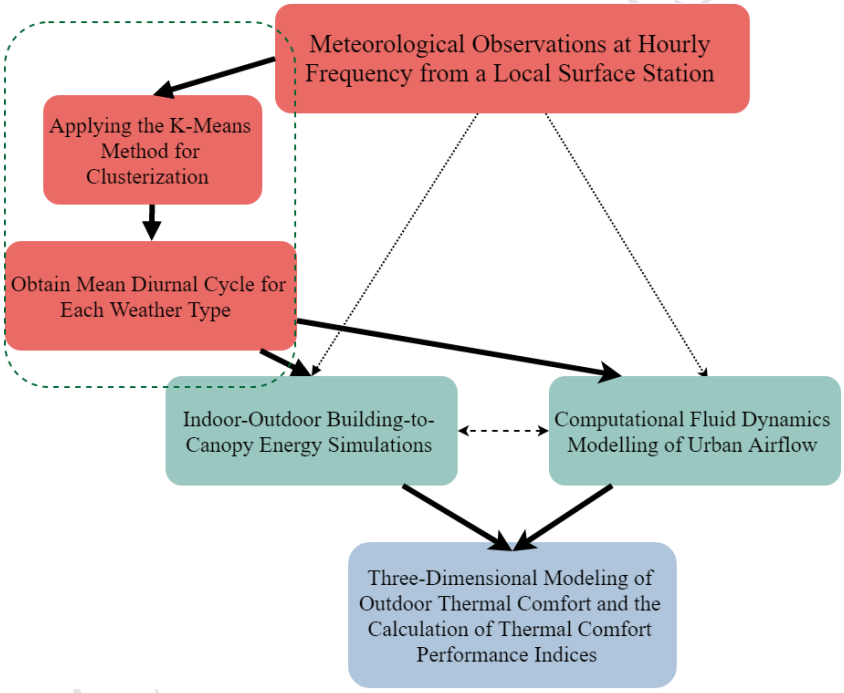

Figure 10: Flow chart of calculating the performance metrics for outdoor thermal comfort analysis. The solid black lines represent the path taken in this analysis, while the dashed/dotted lines represent the alternative or complementary modeling methods: the dotted lines indicate the use of representative weather data at each hour for an entire year (i.e. without clustering) and the dashed line indicates the dynamic coupling of urban energy balance and flow modeling. Here, the energy balance modeling is done using the Temperature of Urban Facets Indoor-Outdoor Building Energy Simulator (TUF-IOBES [63] and [27]), while the flow field is taken from large-eddy simulations (LES) of Nazarian et al. [35]. See Nazarian et al. [37] for more information on the OTC modeling in 3D.

The simulation test case presented here is an idealized array of buildings with plan area density (λ_p) of 0.0625 (demonstrated in Fig. 5) representing sparsely built local climate zones [56]. The energy balance model is run for 10 days encompassing the selected simulation date for each weather type (Table 2) and

the first three days are discarded to avoid the errors associated with the initial boundary conditions. The wind flow simulations are done for a neutral condition with a constant wind direction and wind speed at the forcing height, and then linearly scaled using the hourly wind speed values represented in each weather data. The assumptions are that 1) the effect of thermal forcing on the urban flow field is negligible and b) for the same urban flow regime (isolated buildings [40] here), the flow field at the pedestrian level is linearly correlated with the wind speed at a forcing height. These considerations are due to the limitations regarding the computational costs and acceptable as the present example is only meant for demonstrating the methodology. For a more accurate analysis, however, a one-way (static) or two-way (dynamic) coupling of thermal forcing with flow fields are recommended, which are more feasible to obtain using the weather clustering method presented here as the computational costs are significantly reduced.

For the calculation of the thermal comfort distribution at the pedestrian level, the Outdoor Thermal Comfort in 3D (OTC3D introduced by Nazarian et al. [34, 37]) is used with inputs from a) meteorological forcing data for each weather type (including hourly values of GHI, DNI, DHI, RH, CC, WS), b) 3D distribution of surface temperature from the energy balance model, and c) 3D distribution of wind flow obtained from CFD simulations. SET is taken as the OTC metric and calculated for a standing male pedestrian (metabolic rate = 1.2) who weighs 70 kg, is 150cm tall, and is wearing light summer clothing (iclo=0.34). The skin wetness, body emissivity, and body albedo are considered to be 0.088, 0.95, 0.3, respectively, and the OTC performance metrics are calculated for an outdoor space with operational hours of 0900 (h_i) to 1800 (h_f) local time while the acceptable OTC range (A) is set to 20-28°C.

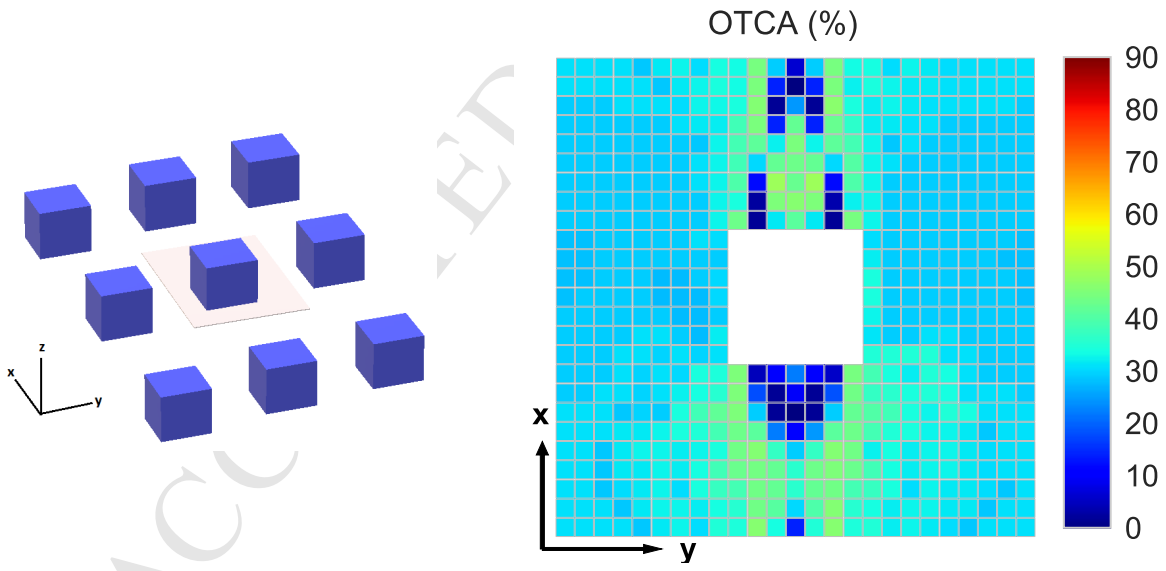

Figure 11: Left: Schematic of a 3D array of idealized buildings with $\lambda_p = 0.0625$. Right: Spatial distribution of OTCA calculated on an annual basis using the clustered weather types. OTCA is calculated at the pedestrian height (1.5m above ground level).

Figure 11 demonstrates the spatial distribution of OTCA (%) calculated for an idealized urban configuration, which is obtained by calculating the OTCA map for each clustered weather type (Fig. 12) and weighing the results based on the frequency of occurrence of weather types throughout the year (Table 2). The high

spatial variability of OTCA at the pedestrian height is seen for all cases in Fig. 12 and the OTCA range is significantly different across various weather types. The spatial variability of OTCA is dominated by two main factors: 1) airflow distribution, and 2) shading pattern at the pedestrian height. In these calculations, the wind direction is aligned with the x-axis (Fig. 11), which is projected in the variability of OTCA around the building for all weather types. The distribution of the shading pattern as well as the shade-to-sunlit area, on the other hand, are dominated by the day of the year for which the simulations are conducted.

In order to better grasp the contributing factors to OTCA, the boxplot distribution of various parameters is also presented in Fig. 13. The critical parameters contributing to thermal comfort (presented as SET here) are a) air temperature, b) wind speed, c) relative humidity, and d) mean radiant temperature. In Fig. 13, these parameters are represented as the spatially-averaged values in each boxplot (i.e. each box plot distribution represents 24 values corresponding to the spatially-averaged values at each hour). For OTCA, however, the boxplot represents the spatial distribution at the pedestrian height, while the consideration of the temporal variabilities is inherent to the OTCA calculations. We observe that the distribution of OTCA is influenced by the combination of meteorological factors, which may have counteracting impacts on OTC at certain hours. Additionally, the day of the simulation determines the sun path, and consequently shading pattern and shade-to-sunlit ratio, which are critical in the spatial distribution of mean radiant temperature as well as OTCA. These factors will further be altered by urban configuration and design elements (that are kept constant here). This analysis further demonstrates that the comprehensive evaluation of OTC performance in an outdoor space needs to consider both spatial and temporal variabilities in contributing (meteorological and design) factors and represents the weather clustering method as an effective method of achieving this objective.

Overall, such maps of OTC performance obtained on an annual basis can be employed for informing the design decisions in the built environment. For example, the persistent zones of adverse thermal comfort shown in this example can be ameliorated by using passive cooling systems such as shading devices, or in the absence of such measures, the recommended use of the outdoor amenities can be limited. Nonetheless, we note that the results presented here are meant as the demonstration of the prescribed methodology and may not represent the final analysis for the case study of Singapore.

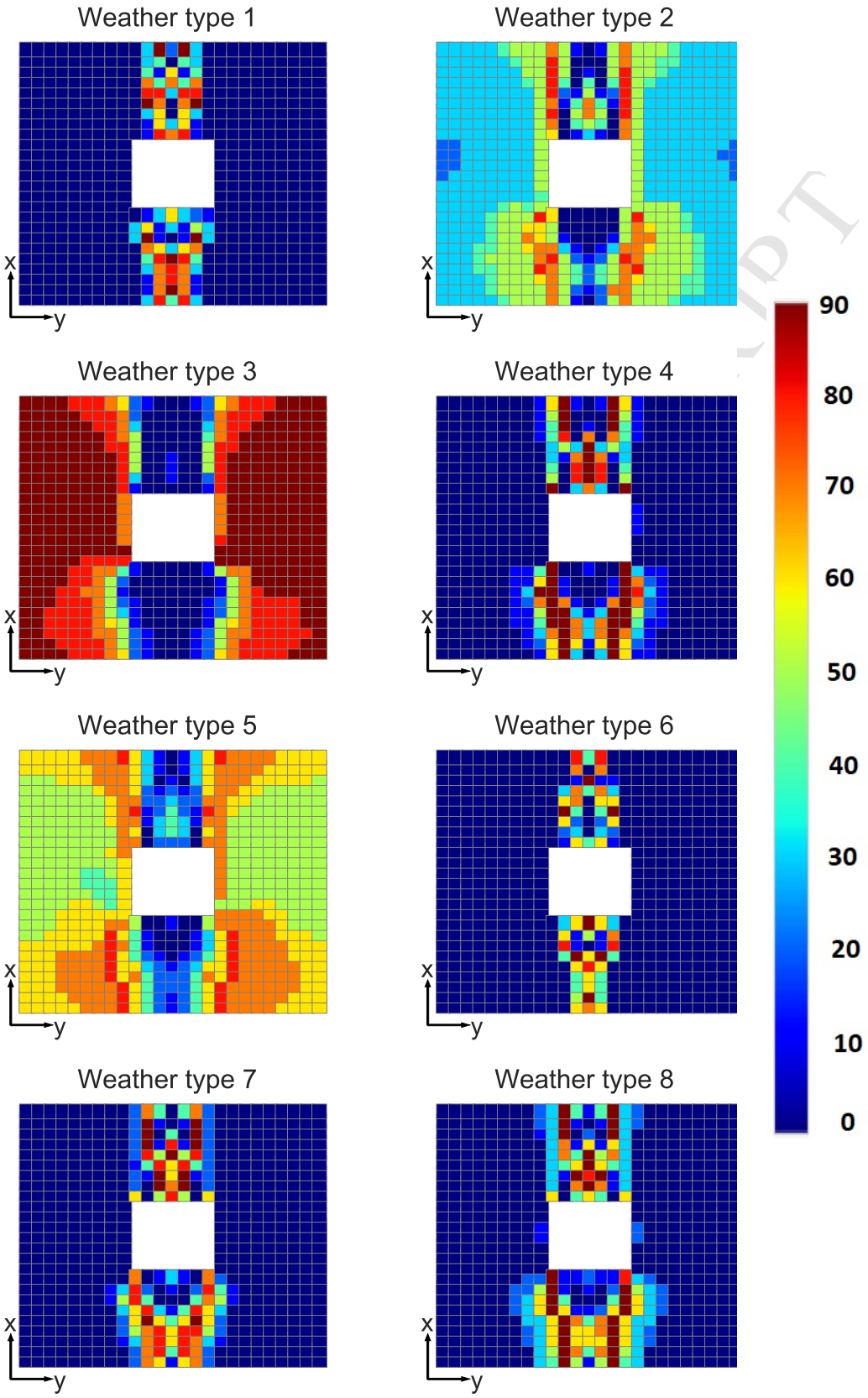

Figure 12: The spatial distribution of OTCA (%) at the pedestrian height ($\lambda_p = 0.0625$ shown in Fig. 11) for the different weather types represented in Table 2 and Appendix B. The color scale (shown in right) is kept consistent for all plots.

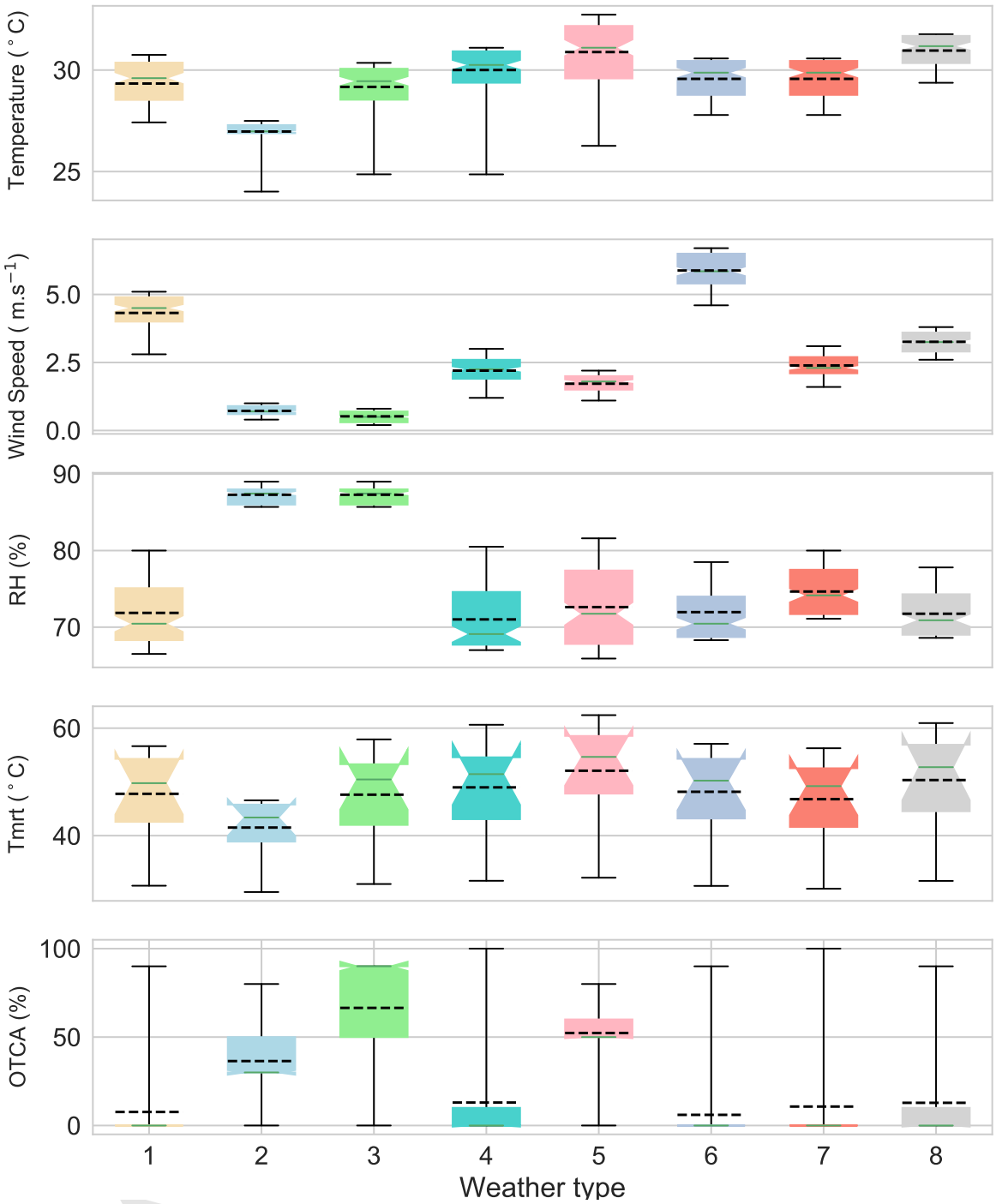

Figure 13: The notched boxplot distribution of hourly environmental parameters (such as air temperature, wind speed, and relative humidity - spatially averaged), hourly mean radiant temperature (T_{mrt} - spatially averaged), and the resulting spatial distribution of OTCA for each weather type (indicated in Table 2). The box shows the Inter-Quartile Range (IQR), that is the 25 to 75 percentile, that covers 50% of the data points. The whiskers are then extended to the minimum and maximum values. The horizontal green line and notch in the box plot indicate the median and the 95% confidence interval around the median, respectively, while the dashed black line is the arithmetic averaged. In the boxplot of T_{mrt} data, the distribution of data is skewed and the 95% confidence internal overlaps with the 75th percentile (3rd quartile), which explains the representation of the box.

5 Discussions regarding the use of comfort indices

In the present study, the performance metrics are calculated using the thermal comfort index SET. Here, we extend the discussion to consider other commonly-used comfort and heat stress indices. A recent comprehensive review of thermal comfort studies by Potchter et al. [46] reveals that out of 165 human thermal indices that have been developed, the most used indices for outdoor thermal perception studies are PET, PMV, UTCI, SET, and WGBT. Table 3 compares the range and descriptions of thermal sensation for these indices in addition to Wind Chill Temperature (WCT). For the indices that are based on the energy balance of human body, such as PET, SET, and UTCI, and described in temperature units, the calculation of OTCA and other performance metrics are as described before: First, the "thermal comfort acceptability criteria," i.e. the thermal comfort range that describes the desirable OTC conditions at a specific outdoor space, is selected based on the thermal comfort index, and further calibrated based on the local climate as well as the desired use of the outdoor space. For example, in the case of Singapore, the acceptable thermal comfort range for a general-use outdoor space and based of SET calculations is found to be 20 to 28° [54, 64]. Using this range, the OTCA map as well as the spatial and continuous OTCA values can be calculated. Second, the critical temperature difference (Eq. 6) should be determined for the calculation of the Thermal Stress Indicator (i.e. the average deviation of comfort index from the acceptable criteria), weighted OTCA, and the frequency of the events outside of the acceptable criteria. The critical temperature difference is directly related to the acceptable range, but can further be modified to indicate the thermal stress zones. Accordingly, similar to the definition of WGBT, the deviation from the "comfortable" range prescribed by ΔT_{ave} can be classified in zones of low, moderate, high, and extreme stress. For the comfort indices differently prescribed, such as PMV, however, the calculation of critical temperature difference requires further investigation.

Table 3: Comparing thermal sensation based on various bioclimatic comfort/stress indices. The thermal sensation at each scale are taken from WGBT, WCT, and UTCI alert descriptions.

	Thermal Comfort Indices					
Thermal Sensation	PET	UTCI	SET	PMV	WGBT	WCT
Frosty (extreme hazard/Very strong cold stress)		-40 to -27				<-55
Very cold (very cold/Strong cold stress)	4	-27 to -30		-3		-54 to -40
Cold (cold/Moderate cold stress)	4 to 8	-13 to 0		-2		-39 to -28
Cool (moderate hazard/Slight cold stress)	8 to 18	0 to 9	<17	-1		-27 to -10
Comfortable (no danger/No thermal stress)	18 to 23	9 to 26	17 to 30	0	<18	>-10
Warm (caution/Moderate heat stress)	23 to 35	26 to 32	30 to 34	1	18 to 24	-
Hot (extreme caution/Strong heat stress)	35 to 41	32 to 38	34 to 37	2	24 to 28	-
Very hot (danger/Very strong heat stress)	>41	38 to 46	>37	3	28 to 30	-
Sweltering (extreme danger/Extreme heat stress)		>46			>30	-

6 Conclusions

For achieving climate-conscious urban design, comprehensive, accurate, and easily comprehensible evaluations of OTC are needed, such that the knowledge obtained from climatological assessments intersects the fields of architecture and urban planning. To respond to this need, we propose the first detailed description of metrics that quantify the performance of an outdoor space with regards to thermal comfort and heat stress. Analogous to "daylight autonomy", widely used for indoor urban design [47], the concept of "Outdoor Thermal Comfort Autonomy" is introduced here, which evaluates if the available ambient and design resources are sufficient for an outdoor environment to be thermally comfortable or whether an adaptation strategy is needed. Additionally, the autonomy metrics are tailored to the unique characteristics of thermal comfort in an outdoor space, identifying the extent of deviation from the thermal comfort acceptability range as the Thermal Stress Indicator.

The proposed methodology for assessing the OTC performance through autonomy metrics does not intend to define a new thermal comfort index, but rather presents the means of translating the thermal comfort analyses using current indices into performance evaluations. The performance metrics discussed here introduce a comparative way of assessing design, identifying adaptation strategies, and facilitating climate-conscious decisions. We attempt to a) link human comfort to climate, urban fabric and design, and operation of an outdoor space, b) integrate the high spatial variability of thermal comfort with the diurnal and seasonal patterns in outdoor environments, and c) provide a rich visual feedback that can aid the decision-making process for urban design. Therefore, the methodology that is discussed here is representative of both performance metrics and design process as "the change in mental framework can inform a change in procedure" [30].

The use of performance metrics, such as OTCA, as design goals can enhance the communication of results and bridge the gap between scientific assessment and design decisions, and potentially aid the policy making in urban environments. Accordingly, the primary benefits of such urban design analysis include:

- Comprehensive metric for integrating spatial, temporal, and behavioral (such as occupancy hour and desirable comfort range) factors. The key advantage of dynamic performance metrics is that they consider the quantity and character of daily and seasonal variations of OTC for a given outdoor site together with irregular meteorological events.
- Comparative metric for assessing the adaptation and mitigation strategies. The use of a visual representation and simplified methods of communicating the results aids a holistic comparison of various adaptation and mitigation strategies proposed for enhancing thermal comfort in outdoor spaces.
- Quantitative metric for rethinking assumptions. While the final communication of results is simple and intuitive, the detailed consideration of various factors allows us to address various assumptions and complicated interactions in both urban design and assessment methodologies.

The contribution of this study goes beyond the definition of the performance metrics for OTC. In order to enable the scientists, designers, and architects to fully implement these metrics, we further discuss how to obtain comprehensive, accurate, yet efficient calculations. By discussing the limitation of the current microclimate models, we draw attention to critical factors, such as the 3D distribution of airflow in the

built environment and realistic shading patterns, which should be scrutinized for an accurate evaluation of OTC performance. Additionally, we discuss weather clustering as an effective method for minimizing the computational cost and complexities of calculating OCT performance, while not jeopardizing the important variabilities in meteorological conditions throughout the year. In this way, we believe that the users not only have the right tools for assessment, but would know how to use them efficiently and accurately.

The presented work describes the framework of evaluating the thermal comfort performance in outdoor spaces that is first of its kind. However, certain limitations persist which are left for future works for enhancing the analysis:

- There is a need for more comprehensive sensitivity analyses on the role of urban density, material properties, and methodological assumptions on OTCA calculations. For instance, this methodology can be applied in a range of different local climate zones [56] to demonstrate the intra-urban variability in OTC performance, as well as assessing the impact of various mitigation strategies at various LCZs. Additionally, the variability in OTC performance based on environmental parameters and various climatic conditions can be assessed in future research.
- In the present discussion, transient behavior of pedestrians, and the subsequent effects on thermal comfort, is not considered in the definition of performance metrics. Given that pedestrians are more often moving through the outdoor spaces rather than staying for long periods, future research should expand on the performance criteria that also includes a "temporal window" of comfort acceptability.
- The calculation of OTCA can further be extended for using not only "typical" but also "extreme" meteorological condition for current and future scenarios. This methodology can be linked with the measurement data, or the outcome of micro-/ and meso-scale (nested) modeling that predict extreme heat events or future scenarios, and further translate the results into OTC performance metrics in the face of such extreme events.
- In the present analysis, the measured data from the airport station in Singapore is used at the forcing height above the urban canyon, while it is widely acknowledged that the recordings should be translated into forcing data at urban area. If such measurements are not available, it is recommended to use numerical models such as Urban Weather Generator [6] or similar to obtain the meteorological conditions at urban sites.

Acknowledgements

Funding was received from the National Research Foundation Singapore under its Campus for Research Excellence and Technological Enterprise programme.

References

[1] Acero, J. A., Koh, E. J., Pignatta, G., and Norford, L. (2018). Clustering weather types for urban outdoor thermal comfort evaluation in a tropical area. *In Review*.

[2] Ali-Toudert, F. and Mayer, H. (2006). Numerical study on the effects of aspect ratio and orientation of an urban street canyon on outdoor thermal comfort in hot and dry climate. *Building and Environment*, 41(2):94–108.

[3] Ali-Toudert, F. and Mayer, H. (2007). Effects of asymmetry, galleries, overhanging facades and vegetation on thermal comfort in urban street canyons. *Solar Energy*, 81(6):742–754.

[4] Auliciems, A. and Szokolay, S. V. (1997). Thermal comfort. Brisbane. Passive and Low Energy Architecture International (PLEA), University of Queensland.

[5] Baccini, M., Biggeri, A., Accetta, G., Kosatsky, T., Katsouyanni, K., Analitis, A., Anderson, H. R., Bisanti, L., D'ippoliti, D., Danova, J., et al. (2008). Heat effects on mortality in 15 European cities. *Epidemiology*, 19(5):711–719.

[6] Bueno, B., Norford, L., Hidalgo, J., and Pigeon, G. (2013). The urban weather generator. *Journal of Building Performance Simulation*, 6(4):269–281.

[7] Carlucci, S. and Pagliano, L. (2012). A review of indices for the long-term evaluation of the general thermal comfort conditions in buildings. *Energy and Buildings*, 53:194–205.

[8] Chen, L. and Ng, E. (2012). Outdoor thermal comfort and outdoor activities: A review of research in the past decade. *Cities*, 29(2):118–125.

[9] Chow, W. and Heng, S. L. (2018). How 'hot' is too hot? Evaluating acceptable ranges of outdoor thermal comfort in an equatorial urban park. In *25th AMOS National Conference and 12th International Conference for Southern Hemisphere Meteorology and Oceanography, AMOS-ICSHMO 2018*, page 326.

[10] Chow, W. T., Akbar, S. N. B. A., Heng, S. L., and Roth, M. (2016). Assessment of measured and perceived microclimates within a tropical urban forest. *Urban Forestry & Urban Greening*, 16:62–75.

[11] De Dear, R. J. and Brager, G. S. (1998). Developing an adaptive model of thermal comfort and preference/discussion. *ASHRAE transactions*, 104:145.

[12] De Dear, R. J. and Brager, G. S. (2002). Thermal comfort in naturally ventilated buildings: revisions to ashrae standard 55. *Energy and Buildings*, 34(6):549–561.

[13] Fanger, P. (1967). Calculation of thermal comfort: Introduction of a basic comfort equation. *ASHRAE Transactions*, 73:III4.1–III4.20.

[14] Fiala, D., Havenith, G., Bröde, P., Kampmann, B., and Jendritzky, G. (2012). UTCI-Fiala multi-node model of human heat transfer and temperature regulation. *International journal of biometeorology*, 56(3):429–441.

[15] Gagge, A. P., Stolwijk, J. A. J., and Nishi, Y. (1971). An effective temperature scale based on a simple model of human physiological regulatory response. *ASHRAE Transactions*, 77(2192):247–262.

[16] Givoni, B. (1963). *Estimation of the effect of climate on man: Development of a new thermal index*. Hebrew University, Jerusalem.

[17] Hidalgo, J., Masson, V., and Baehr, C. (2014). From daily climatic scenarios to hourly atmospheric forcing fields to force soil-vegetation-atmosphere transfer models. *Frontiers in Environmental Science*, 2:40.

[18] Hoffmann, P. and Schlünzen, K. H. (2013). Weather pattern classification to represent the urban heat island in present and future climate. *Journal of Applied Meteorology and Climatology*, 52(12):2699–2714.

[19] Höppe, P. (1999). The physiological equivalent temperature–a universal index for the biometeorological assessment of the thermal environment. *International journal of Biometeorology*, 43(2):71–75.

[20] Höppe, P. (2002). Different aspects of assessing indoor and outdoor thermal comfort. *Energy and Buildings*, 34(6):661–665.

[21] Huth, R., Beck, C., Philipp, A., Demuzere, M., Ustrnul, Z., Cahynová, M., Kyselỳ, J., and Tveito, O. E. (2008). Classifications of atmospheric circulation patterns. *Annals of the New York Academy of Sciences*, 1146(1):105–152.

[22] Hwang, R.-L., Lin, T.-P., and Matzarakis, A. (2011). Seasonal effects of urban street shading on long-term outdoor thermal comfort. *Building and Environment*, 46(4):863–870.

[23] Johansson, E., Thorsson, S., Emmanuel, R., and Krüger, E. (2014a). Instruments and methods in outdoor thermal comfort studies – The need for standardization. *Urban Climate*, 10:346–366.

[24] Johansson, E., Thorsson, S., Emmanuel, R., and Krüger, E. (2014b). Instruments and methods in outdoor thermal comfort studies–the need for standardization. *Urban Climate*, 10:346–366.

[25] Konstantzos, I. and Tzempelikos, T. (2015). Design recommendations for perimeter office spaces based on visual performance criteria. In *Proceedings of International Conference CISBAT 2015 Future Buildings and Districts Sustainability from Nano to Urban Scale*, number EPFL-CONF-213325, pages 271–276. LESO-PB, EPFL.

[26] Kovats, R. S. and Hajat, S. (2008). Heat stress and public health: a critical review. *Annual Review of Public Health*, 29:41–55.

[27] Krayenhoff, E. S. and Voogt, J. A. (2007). A microscale three-dimensional urban energy balance model for studying surface temperatures. *Boundary-Layer Meteorology*, 123(3):433–461.

[28] Krüger, E., Drach, P., Emmanuel, R., and Corbella, O. (2013). Urban heat island and differences in outdoor comfort levels in Glasgow, UK. *Theoretical and Applied Climatology*, 112(1-2):127–141.

[29] Lai, D., Guo, D., Hou, Y., Lin, C., and Chen, Q. (2014). Studies of outdoor thermal comfort in northern china. *Building and Environment*, 77:110–118.

[30] Levitt, B., Ubbelohde, M., Loisos, G., and Brown, N. (2013). Thermal autonomy as metric and design process. In *CaGBC National Conference and Expo: Pushing the Boundary–Net Positive Buildings*, pages 47–58.

[31] Lin, B., Li, X., Zhu, Y., and Qin, Y. (2008). Numerical simulation studies of the different vegetation patterns' effects on outdoor pedestrian thermal comfort. *Journal of Wind Engineering and Industrial Aerodynamics*, 96(10):1707–1718.

[32] Lin, T.-P., Matzarakis, A., and Hwang, R.-L. (2010). Shading effect on long-term outdoor thermal comfort. *Building and Environment*, 45(1):213–221.

[33] Meteorological Service of Singapore (2017). Annual climatological report. Technical report, Meteorological Service of Singapore, Singapore.

[34] Nazarian, N., Fan, J., Sin, T., Norford, L., and Kleissl, J. (2017a). Predicting outdoor thermal comfort in urban environments: A 3D numerical model for standard effective temperature. *Urban Climate*, 20:251–267.

[35] Nazarian, N., Martilli, A., and Kleissl, J. (2017b). Impacts of realistic urban heating, part I: Spatial variability of mean flow, turbulent exchange and pollutant dispersion. *Boundary-Layer Meteorology*, pages 1–27.

[36] Nazarian, N., Martilli, A., Norford, L., and Kleissl, J. (2018a). Impacts of realistic urban heating. part II: Air quality and city breathability. *Boundary-Layer Meteorology*, 168(2):321–341.

[37] Nazarian, N., Sin, T., and Norford, L. (2018b). Numerical modeling of outdoor thermal comfort in 3D. *Urban Climate*, 26:212–230.

[38] Nicol, J. F. and Humphreys, M. A. (2002). Adaptive thermal comfort and sustainable thermal standards for buildings. *Energy and Buildings*, 34(6):563–572.

[39] Nikolopoulou, M., Baker, N., and Steemers, K. (2001). Thermal comfort in outdoor urban spaces: understanding the human parameter. *Solar energy*, 70(3):227–235.

[40] Oke, T. R. (1988). Street design and urban canopy layer climate. *Energy and Buildings*, 11(1):103–113.

[41] Park, M., Hagishima, A., Tanimoto, J., and Narita, K.-i. (2012). Effect of urban vegetation on outdoor thermal environment: field measurement at a scale model site. *Building and Environment*, 56:38–46.

[42] Perkins, S., Alexander, L., and Nairn, J. (2012). Increasing frequency, intensity and duration of observed global heatwaves and warm spells. *Geophysical Research Letters*, 39(20).

[43] Philipp, A., Bartholy, J., Beck, C., Erpicum, M., Esteban, P., Fettweis, X., Huth, R., James, P., Jourdain, S., Kreienkamp, F., et al. (2010). Cost733cat–a database of weather and circulation type classifications. *Physics and Chemistry of the Earth, Parts A/B/C*, 35(9-12):360–373.

[44] Philipp, A., Della-Marta, P.-M., Jacobeit, J., Fereday, D. R., Jones, P. D., Moberg, A., and Wanner, H. (2007). Long-term variability of daily north atlantic–european pressure patterns since 1850 classified by simulated annealing clustering. *Journal of Climate*, 20(16):4065–4095.

[45] Pickup, J. and de Dear, R. (2000). An outdoor thermal comfort index (OUT_SET*): the model and its assumptions. In *Biometeorology and urban climatology at the turn of the millenium. Selected Papers from the Conference ICB-ICUC*, volume 99, pages 279–283.

[46] Potchter, O., Cohen, P., Lin, T.-P., and Matzarakis, A. (2018). Outdoor human thermal perception in various climates: A comprehensive review of approaches, methods and quantification. *Science of the Total Environment*, 631:390–406.

[47] Reinhart, C. F., Mardaljevic, J., and Rogers, Z. (2006). Dynamic daylight performance metrics for sustainable building design. *Leukos*, 3(1):7–31.

[48] Roth, M. and Chow, W. T. (2012). A historical review and assessment of urban heat island research in singapore. *Singapore Journal of Tropical Geography*, 33(3):381–397.

[49] Roy, A. (2015). India heat wave kills 1,500 in taste of climate change impacts. *Climate Home*.

[50] Rupp, R. F., Vásquez, N. G., and Lamberts, R. (2015). A review of human thermal comfort in the built environment. *Energy and Buildings*, 105:178–205.

[51] Salata, F., Golasi, I., de Lieto Vollaro, R., and de Lieto Vollaro, A. (2016). Outdoor thermal comfort in the Mediterranean area. a transversal study in rome, italy. *Building and environment*, 96:46–61.

[52] Shashua-Bar, L., Pearlmutter, D., and Erell, E. (2011). The influence of trees and grass on outdoor thermal comfort in a hot-arid environment. *International Journal of Climatology*, 31(10):1498–1506.

[53] Shen, J., Chang, S. I., Lee, E. S., Deng, Y., and Brown, S. J. (2005). Determination of cluster number in clustering microarray data. *Applied Mathematics and Computation*, 169(2):1172–1185.

[54] Song, J. (2006). *Thermal comfort for semi-outdoor spaces in the tropics*. PhD thesis, Department of Building, National University of Singapore.

[55] Spagnolo, J. and De Dear, R. (2003). A field study of thermal comfort in outdoor and semi-outdoor environments in subtropical Sydney australia. *Building and environment*, 38(5):721–738.

[56] Stewart, I. D. and Oke, T. R. (2012). Local climate zones for urban temperature studies. *Bulletin of the American Meteorological Society*, 93(12):1879–1900.

[57] Taleghani, M., Kleerekoper, L., Tenpierik, M., and van den Dobbelsteen, A. (2015). Outdoor thermal comfort within five different urban forms in the netherlands. *Building and Environment*, 83:65–78.

[58] Thom, J. K., Coutts, A. M., Broadbent, A. M., and Tapper, N. J. (2016). The influence of increasing tree cover on mean radiant temperature across a mixed development suburb in Adelaide, australia. *Urban forestry & urban greening*, 20:233–242.

[59] Thorsson, S., Lindberg, F., Björklund, J., Holmer, B., and Rayner, D. (2011). Potential changes in outdoor thermal comfort conditions in gothenburg, sweden due to climate change: the influence of urban geometry. *International Journal of Climatology*, 31(2):324–335.

[60] Tung, C.-H., Chen, C.-P., Tsai, K.-T., Kántor, N., Hwang, R.-L., Matzarakis, A., and Lin, T.-P. (2014). Outdoor thermal comfort characteristics in the hot and humid region from a gender perspective. *International journal of biometeorology*, 58(9):1927–1939.

[61] Wiltgen, N. (2015). Tokyo Heat Wave Lasted Eight Days, Doubling All-Time Record; 55 Confirmed Dead in Japan. *The Weather Channel*.

[62] Xu, Z., FitzGerald, G., Guo, Y., Jalaludin, B., and Tong, S. (2016). Impact of heatwave on mortality under different heatwave definitions: a systematic review and meta-analysis. *Environment international*, 89:193–203.

[63] Yaghoobian, N. and Kleissl, J. (2012). Effect of reflective pavements on building energy use. *Urban Climate*, 2:25–42.

[64] Yang, W., Wong, N. H., and Jusuf, S. K. (2013). Thermal comfort in outdoor urban spaces in Singapore. *Building and Environment*, 59:426–435.

[65] Zhang, F., de Dear, R., and Hancock, P. (2019). Effects of moderate thermal environments on cognitive performance: A multidisciplinary review. *Applied Energy*, 236:760–777.

[66] Zomorodian, Z. S. and Tahsildoost, M. (2017). Assessment of window performance in classrooms by long term spatial comfort metrics. *Energy and Buildings*, 134:80–93.

APPENDICES

Appendix A - Specification of K-Means Method used for Clustering

The statistical k-means method has been applied to cluster weather types in Singapore. This method is based on the Squared Euclidean Distance (SED) between two data objects that can include one or more variables. The algorithm looks for the minimum value of the so-called "Within-cluster Sum of Squares (WSS)" defined as the sum of the squared differences between the observations and the corresponding centroid [43]:

$$\mathrm{WWS} = \sum_{\mathrm{i}=1}^{\mathrm{k}} \sum_{\mathrm{x}\in \mathrm{C_i}} ||\mathrm{x} - \mathrm{z_i}||^2 \tag{11}$$

where x denotes all the data belonging to the cluster C_i, z_i is the ith corresponding Cluster Centroid (CC) and k is the number of clusters. The minimum WWS is obtained in an interactive process that starts with the selection of CCs. The SED is calculated for each combination of CC and data objects. All data objects are assigned to their nearest CC to form the cluster. Data objects of each cluster are averaged to provide a new CC. This procedure of CC reassignment and calculation of SED ends when no data needs to be reassigned to another CC. The final CCs are unique for each cluster and represent all the data objects contained.

For the selection of the optimal number of clusters in which the yearly meteorological data should be divided, we have used the Dynamic Validity Index ($DVIndex$) developed by Shen et al. [53]. It is based on the assumption that clusters should be compact and well separated from each other. This is represented by the minimum value of $DVIndex$.

For each cluster k, the DVIndex is defined as

$$DVIndex(k) = IntraRatio(k) + \gamma InterRatio(k) \tag{12}$$

where

$$IntraRatio(k) = \frac{Intra(k)}{MaxIntra} \ , \tag{13}$$

$$InterRatio(k) = \frac{Inter(k)}{MaxInter} \ , \tag{14}$$

$$Intra(k) = \frac{1}{N} \sum_{i=1}^{k} \sum_{x \in C_i} ||x - z_i||^2 \ , \tag{15}$$

$$Inter(k) = \frac{Max_{i,j}(||z_i - z_j||^2)}{Min_{i \neq j}(||z_i - z_j||^2)} \sum_{i=1}^{k} \left(\frac{1}{\sum_{j=1}^{k}(||z_i - z_j||^2)}\right) \ , \tag{16}$$

$$MaxIntra = \max_{i=1,\ldots,K}(Intra(i)), \text{ and} \tag{17}$$

$$MaxInter = \max_{i=1,\ldots,K}(Inter(i)) \ . \tag{18}$$

Here, N is the number of data objects to be clustered, K is the pre-defined upper bound number of clusters (20 in our case), z_i is the CC of the cluster C_i, and γ is a tuning parameter (0.5) taken from Hoffmann and Schlünzen [18].

Appendix B - Clustered Weather Types Obtained for Singapore

The clusters have been defined using the following variables: daily mean temperature, daily mean temperature amplitude, daily mean vapour pressure, daily mean global incoming radiation, and mean u - v wind components. These daily values were obtained from the EnergyPlus Weather data (EPW file extention) that represents an hourly dataset of a typical meteorological year of Singapore. Fig. B.1 demonstrates the DVIndex for different numbers of clusters obtained using the k-means clustering procedure (detailed in Appendix A). The minimum DVIndex value corresponds to the eight clusters that were selected as the weather types.

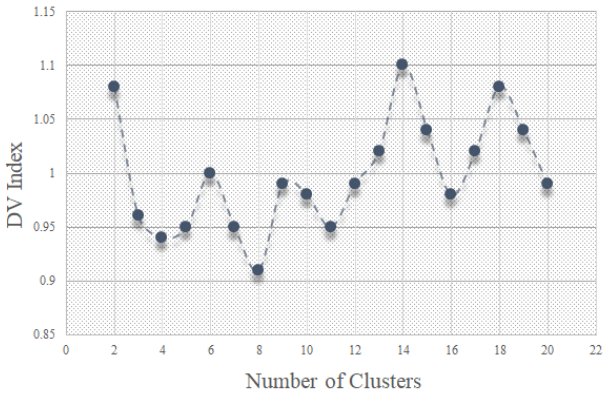

Figure B.1: DVIndex (Eq. 12) calculated for different number of clustered weather types.

Quantitative measures of the performance of the clustering procedure are presented in Table B.1. The best performance is for air temperature, relative humidity, and global incoming radiation. Although the Pearson correlation coefficient (R^2) is lower for the rest of the variables, the root mean square error (RMSE) presents acceptable values for a yearly thermal comfort analysis.

Table B.1: Quantitative measures of clustered hourly variables with respect to EPW file (on an hourly basis) for Singapore

Microclimate parameter	R^2	RMSE
Air Temperature (T_a)	0.706	1.2
Relative Humidity (RH)	0.686	5.7
Global Horizontal Irradiance (GHI)	0.930	68.8
Wind Speed (u-component)	0.565	1.5
Wind Speed (v-component)	0.422	1.2

Figure B.2 shows the diurnal variation in each of the clustered weather types for the variables that are relevant to the modelling of thermal comfort (see Sec. 4.1.1). The diurnal variations are well represented compared to the weather conditions in Singapore. For example, weather type 1 represents an overcast day with lowest daily maximum temperature (26.8 °C) and lowest global incoming radiation (negligible direct solar radiation) in Singapore. Wind speed is low (associated to calm conditions) and wind direction is from NE especially during the afternoon. Relative humidity values corresponds to the highest recorded value

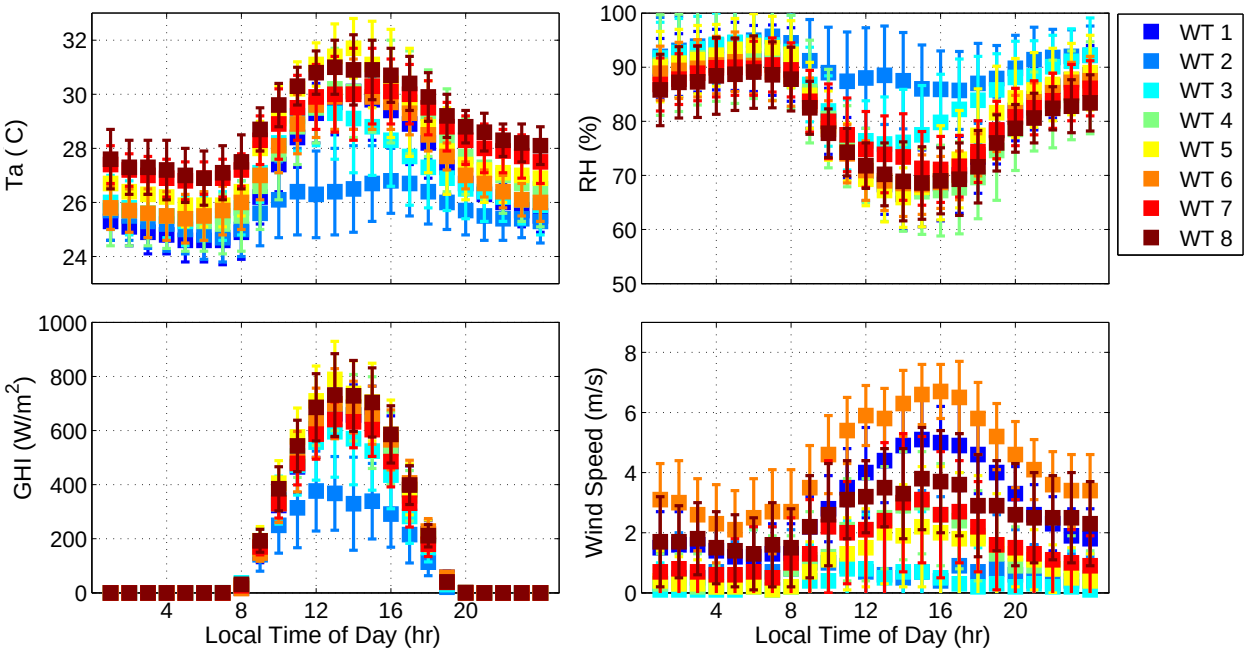

Figure B.2: Hourly evolution of air temperature (T_a), relative humidity (RH), global incoming radiation, (GHI), and wind speed for the 8 clustered weather types. The ID number for each weather type (WT) corresponds to Table 2.

in Singapore and precipitation is expected during these days. These climatic characteristics correspond to a typical day in the wet NE monsoon season but could also occur in other seasons. On the whole it represents 10.4% of the days of Singapore. On the contrary, weather type 4 represent a day with high maximum temperatures (31.7 °C) and the highest global radiation (789 $\mathrm{W\,m^{-2}}$) due to low cloud cover. Wind direction is constant from the NE and wind speed increases during daytime to more than 2 $\mathrm{m\,s^{-1}}$. Daytime relative humidity values are low and no precipitation is expected during these days. This conditions are representative of the NE monsoon in the dry period that accounts for 16.7% of the days in Singapore.

Highlights

- Outdoor thermal comfort is critical for livability and should be considered in urban design
- We define 4 quantitative metrics to assess OTC performance in the built environment
- OTC metrics links comfort to urban climate, design, and the space operation
- Thermal Comfort Autonomy provides visual feedback to aid decision-making in urban design
- We observe the role of realistic microclimate representation on the OTC metrics
- We discuss weather clustering to reduce OTCA calculation cost and maintain accuracy